trial [12] in which patients who were disease-free after definitive treatment received oral administration of 600 mg peretinoin daily for one year. The results showed that peretinoin significantly reduced the incidence of recurrent or new HCC [12] and improved patient survival rates [13]. Based on the results of rat pharmacological studies [14,15] and a phase I clinical study of peretinoin [16], a phase II/III clinical study of peretinoin was conducted in which the doses were set at 300 and 600 mg daily. The study demonstrated that, in the Child-Pugh A subgroup, 600 mg/day peretinoin (n=100) reduced the risk of HCC recurrence or death by approximately 40% compared to placebo (n=106) [hazard ratio (HR)=0.60; 95% confidence interval (CI): 0.40–0.89)] [17]. On the other hand, 300 mg daily doses of peretinoin were insufficient for tumor control and showed no substantial difference from the placebo [17]. A large-scale clinical study including several countries is now planned to confirm the clinical efficacy of peretinoin.

Little is known about the mechanism by which peretinoin exerts its inhibitory effects against recurrent HCC in humans *in vivo*. In order to investigate this mechanism, we conducted here a comparative study recruiting HCV-positive patients who successfully completed definitive treatment for HCC (similar to the phase II/III clinical study mentioned above). Patients underwent liver biopsy before and after 8 weeks of treatment with repeated doses of peretinoin, and the collected samples were analyzed for gene expression profiling using the remnant liver after eradication of HCC. We found that changes in the gene expression signature observed in this study help us to understand the means by which peretinoin suppresses HCC, in particular its inhibition against *de novo* carcinogenesis.

Methods

Patients

We enrolled 12 HCV-positive patients who were cured of their primary and first recurrent HCC by surgical hepatectomy or radiofrequency ablation therapy and other non-surgical local treatments (Table 1). Complete tumor removal was confirmed by dynamic computed tomography (CT) scans. Inclusion criteria were as follows: positive presence of HCV-RNA in the serum; Child-Pugh class A or B liver function; platelet counts ≥50,000/μL; and age ≥20 years. Exclusion criteria included the following: positive for hepatitis B surface antigen; tumor infiltration into the portal vein; use of transarterial embolization or transarterial chemoembolization (TAE/TACE) for definitive therapy; postoperative use of investigational medicinal products, antitumor agents, interferon, or vitamin K2 formulations; blood pressure unmanageable even with medication (systolic pressure ≥160 mmHg or diastolic pressure ≥100 mmHg); complication with renal impairment, cardiovascular disease, diabetes mellitus, autoimmune disease, asthma, or other severe disease; presence of neoplasm; allergy to CT contrast media; allergy to retinoids; history of total gastrectomy; possible pregnancy during study; and lactating mothers.

Study design

This trial was a randomized, parallel-group, open-label study. Twelve eligible patients signed the informed consent form for registration. They were randomized to receive one of the two peretinoin doses: 600 or 300 mg per day. Each dose group consisted of 6 patients. After randomization, patients underwent liver biopsy before the start of peretinoin treatment, then orally received peretinoin twice daily for 8 weeks. At the end of the 8-week therapy, they underwent a second liver biopsy (Figure 1A). The collected biopsy samples were kept in RNAlater® solution (Ambion Inc., Austin, TX) at 4°C overnight or longer. Within 3 days, the biopsy samples were removed from the RNAlater solution and partially subjected to RNA extraction and purification. The purified RNA samples were stored at −80°C until required for gene expression profiling. The remaining part of the biopsy samples was used to determine the intrahepatic peretinoin concentration. Samples were placed in polypropylene bottles containing 99.5% ethanol, and the air in the bottle was purged with argon. The bottles were tightly closed and stored at −80°C protected from light. Peripheral blood samples were also collected for the analysis of gene expression signatures and to determine plasma peretinoin levels.

After the second biopsy, patients were orally administered peretinoin twice daily for 88 weeks. During the treatment period, patients visited the hospital every 4 weeks for check-ups, drug compliance, and protocol-specified medical examinations. Drug compliance was assessed by pill counts. During the study, use of anticancer agents, interferon, vitamins K and A, and antiviral drugs (e.g., rivabirin) was prohibited. The study was registered at the Japan Pharmaceutical Information Center (JapicCTI-121757). This protocol was approved by the Institutional Review Board of Kanazawa University for clinical investigation following the provisions of Helsinki, Good Clinical Practice guidelines, local laws, and regulations. Written informed consent was obtained from all patients involved in this study. The detail protocol of this study is presented in Additional file 1: Study protocol.

Plasma peretinoin concentration

A 5-mL blood sample was drawn into an EDTA-2Na tube, immediately mixed, and centrifuged to obtain a plasma sample. The air in the sample tubes was replaced with argon, and the tubes were stored at −80°C protected

Table 1 Patient characteristics and prognosis

Patient no.	Dose	Age	Sex	P/R	Curative treatment	MTD	Tumor no.	Tumor histology	Background liver		CP	ALT	PLT	Prognosis	
									F	A				2 yrs	4.5 yrs
1	300	70	F	P	RFA	15	2	m-p	4	2	A	112	7.9	Rec	Rec
2	600	72	F	R	RFA	20	2	w	4	2	A	40	7.9	Rec	Rec λ
3	300	58	M	P	resection	25	1	m-p	2	1	A	16	19.2	nonRec	nonRec
4	600	54	M	P	resection	25	1	m-p	3	2	A	57	16.4	nonRec	Rec
5	600	60	F	P	RFA	23	1	m-p	4	2	B	23	6.4	nonRec	nonRec
6	300	73	F	P	RFA	20	2	m-p	3	2	A	31	14.2	Rec	Rec λ
7	300	69	F	P	RFA	11	3	w-m	4	1	A	38	11.5	Rec	Rec λ
8	600	74	F	P	RFA	16	2	m-p	4	1	A	45	5.1	nonRec	Rec
9	600	65	M	R	RFA	10	1	m-p	2	1	A	29	16.5	nonRec	nonRec
10	600	59	M	P	resection	34	1	m-p	4	2	B	60	9.4	nonRec	nonRec
11	300	70	F	R	RFA	15	1	w-m	4	2	B	98	7	nonRec	nonRec
12	300	66	M	P	RFA	15	1	m-p	4	1	A	90	10.6	nonRec	nonRec

Dose (mg/day), ALT(U/L), PLT($\times 10^4/\mu L$), MTD (mm).
F; female, M; male, P; primary HCC, R; (first) recurrent HCC, MTD; maximum tumor diameter, w; well-differentiated, m; moderately differentiated, p; poorly differentiated, F; fibrosis stage, A; activity grade, CP; Child-Pugh classification, ALT; alanine aminotransferase, PLT; platelet.
Rec; recurrence, nonRec; non-recurrence, λ; death.

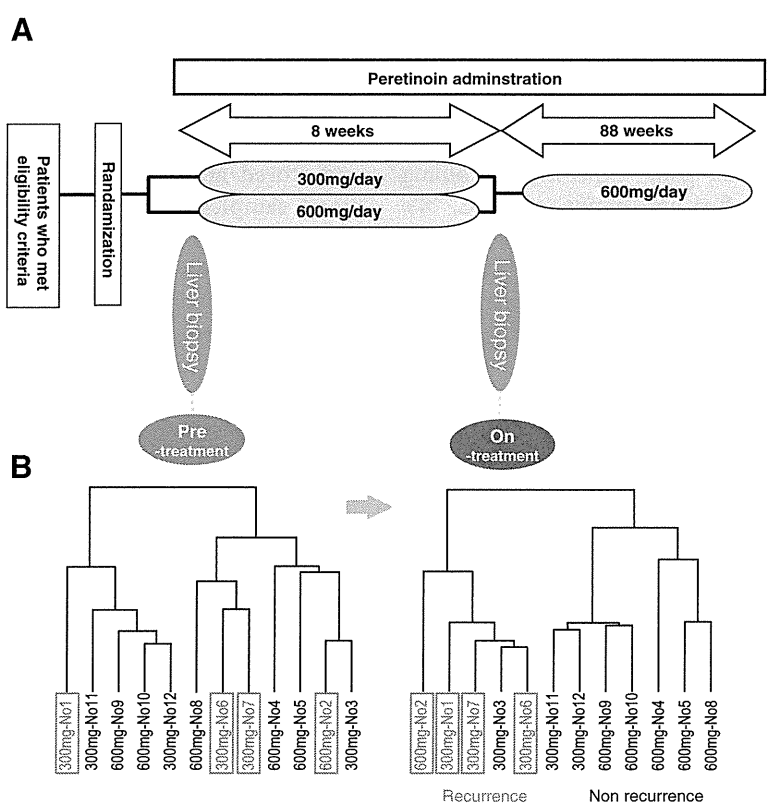

Figure 1 Peretinoin pharmacokinetics study design and change of gene expression profiling. A: Peretinoin pharmacokinetics study design. Twelve patients were enrolled in the study and two groups of 6 patients were randomly administered one of two doses of peretinoin (600 or 300 mg per day) for 8 weeks. A liver biopsy was obtained before the start of peretinoin administration and 8 weeks into the treatment. After the second liver biopsy, oral administration of peretinoin twice daily was resumed for 88 weeks. **B**: Hierarchical clustering analysis of patients using all expressed genes. Patient numbers (Table 1) and peretinoin dose are listed. Patients with HCC recurrence are shown in red and boxed. There was no significant association between hepatic gene expression and HCC recurrence before starting peretinoin treatment, while distinct clusters of patients were observed after week 8 depending on HCC recurrence.

from light. The plasma concentrations of the unchanged form of peretinoin and its lipid-bound form were determined as follows: first, the peretinoin-containing fractions were extracted from the plasma samples, then subjected to derivatization of peretinoin, and the concentration of the derivative was measured by liquid chromatography-atmospheric pressure chemical ionization-tandem mass spectrometry.

Liver peretinoin concentration

Collected liver tissue samples were immersed in 99.5% ethanol in containers, and the internal air was replaced with argon. The samples were stored at −80°C protected from light. The liver concentrations of the unchanged form of peretinoin and its lipid-bound form were determined as for the plasma concentrations above.

Microarray analysis

For gene expression profiling of the liver, in-house cDNA microarrays containing a representative panel of 10,000 liver-specific genes (Kanazawa liver chip 10K ver. 2.0) were used. RNA isolation, amplification of antisense RNA, labeling, and hybridization were conducted as previously described [18].

To identify genetic variants, paired *t*-tests were performed using BRB-Array Tools software (http://linus.nci.nih.gov/BRB-ArrayTools.html) to define *P*-values <0.05 as gene variants. Hierarchical cluster analysis, exploration of significantly expressed genes, and class prediction were also performed using the BRB-Array Tools.

Hierarchical clustering was carried out using centered correlation and average linkage. The class comparison tool in the BRB-Array Tools was used to extract significantly expressed genes. Genes whose expression levels were significantly different between two groups were located by the *t*-test at the $P<0.002$ significance level. Univariate permutation tests were repeated 1,000–2,000 times to control for errors. Class prediction was performed using the above-mentioned significantly differentiated genes as discriminators, and the results were cross-validated using seven algorithms: compound-covariate predictor, diagonal linear discriminant analysis, 1-nearest neighbor, 3-nearest neighbors, nearest centroid, support vector machine, and Bayesian compound covariate. The mean value of the seven success rates for class prediction was defined as the prediction accuracy rate [18].

Pathway analysis was performed using MetaCore™ (Thomson Reuters, New York, NY) and functional ontology enrichment analysis was performed to find differentially expressed pathway using differentially expressed genes [18,19].

The microarray data have been submitted to the Gene Expression Omnibus (GEO) public database at NCBI (Accession No. GSE29302).

Quantitative real-time detection polymerase chain reaction

Quantitative real-time detection polymerase chain reaction (RTD-PCR) was performed using the TaqMan Universal Master Mix (PE Applied Biosystems, Foster City, CA). Primer pairs and probes were purchased from the TaqMan assay reagents library. Standard curves were generated for each assay using RNA derived from normal human liver tissue. Expression data were normalized by GAPDH, and the results are shown as the relative fold expression to the normal liver.

Statistical analysis

Results are expressed as means ± S.D. Significance was tested by one-way ANOVA with Bonferroni's method, and differences were considered statistically significant at $P<0.05$.

Results

Safety

In this study, 88 adverse events were recorded in 12 patients (100%). Major adverse events included rhinopharyngitis (n=7), blood pressure elevation (n=5), peripheral edema (n=3), and enteritis (n=3). Most of these adverse events were mild or moderate, and were adequately controlled. Nine serious adverse events were documented in 5 patients, including hyperglycemia (n=2) and coronary stenosis (n=1). However, all reported serious adverse events were alleviated with appropriate treatment, and there was no substantial concern identified regarding the safety of peretinoin.

Plasma peretinoin concentration

Plasma peretinoin concentrations were determined at week 8 of treatment. The mean (± SD) plasma concentrations of the unchanged form of peretinoin were 82.3 (± 90.0) and 201.2 (± 111.4) ng/mL at 4 h post-dose and 35.8 (± 49.2) and 29.0 (±17.9) ng/mL at 8 h post-dose for the 300 and 600 mg per day groups, respectively. The plasma concentrations of the unchanged peretinoin measured at 4 h post-dose ($\approx t_{max}$) were dose-dependent. The mean (± SD) plasma concentrations of the lipid-bound form of peretinoin were 1478.8 (± 853.7) and 2789.8 (± 1630.0) ng/mL at 4 h post-dose and 1227.8 (± 942.7) and 2213.2 (± 1156.1) ng/mL at 8 h post-dose for the 300 and 600 mg per day groups, respectively. The plasma concentrations of the lipid-bound form of peretinoin were dose-dependent at 4 and 8 h post-dose.

Liver peretinoin concentration

Liver peretinoin concentrations were determined at week 8 of treatment. The measurements of the liver concentration of the unchanged form of peretinoin were all below the lower limit of quantitation at 4 h post-dose for all 6 patients in the 300 mg per day group. For the

600 mg per day group, 2 patients yielded measurements of 0.052 and 0.059 μg/g, while the remaining 4 patients produced results under the lower limit of quantitation (0.050 μg/g). The mean (± SD) concentrations of the lipid-bound form of peretinoin were 13.7508 (± 11.1097) and 12.8345 (± 8.7048) μg/g for the 300 and 600 mg per day groups, respectively.

Gene expression analysis

To analyze the gene expression signature of the liver tissue, we identified genes whose expression levels were significantly different before and after the start of the peretinoin treatment (Figure 1A). The identified genes were candidates for peretinoin-responsive genes. The phase II/III clinical study showed that a daily dose of 600 mg peretinoin reduced the risk of HCC recurrence, while a 300 mg dose was not significantly different from the placebo [17]. Therefore, gene expression patterns were compared before and after the start of the 600 mg peretinoin therapy (n=6). Consequently, 424 hepatic genes showed significantly different expression levels from baseline at week 8 (enhancement and suppression seen for 190 and 234 genes, respectively). Typical examples of these genes are represented in Table 2 where fold changes of gene expression for the 300 mg and 600 mg doses are shown respectively. In addition to the retinoid-induced genes, genes related to interferon, tumor suppressors, negative regulators of Wnt signaling, insulin-like growth factor (IGF) signaling, and hepatocyte differentiation were significantly up-regulated by peretinoin. By contrast, genes related to the mammalian target of rapamycin (mTOR), tumor progression, cell cycle, and metastasis/angiogenesis were down-regulated. Serial changes in peretinoin-responsive gene expression are shown in Additional file 2: Figure S1. Significant changes in expression were observed in response to 600 mg of peretinoin, while changes in expression were minimal with 300 mg of peretinoin.

Hierarchical clustering of patients using hepatic gene expression prior to administering peretinoin revealed no significant association with clinical outcome, but a significant association became clearly apparent 8 weeks after peretinoin treatment (Figure 1B). The patients were clustered into two groups: one containing patients with HCC recurrence (4 of 5 patients had recurrence) and the other containing those without recurrence (all 6 patients were recurrence free) within 2 years. Supervised learning methods using seven different algorithms showed that the patients receiving treatment could be differentiated into two groups with or without recurrence by 224 gene predictors ($P<0.002$) at 79.6% accuracy ($P<0.05$) (Table 3). Interestingly, 44 of 224 (20%) genes were peretinoin induced.

Although peretinoin-responsive genes were more induced in patients treated with the 600 mg dosage, gene expression profiling 8 weeks after peretinoin treatment could not be classified according to the dosage (Table 3). This might be because two patients treated with the 300 mg dosage (No. 11 and No. 12) had already expressed high levels of peretinoin-response genes before starting peretinoin treatment (Additional file 2: Figure S1). Interestingly, patients with high levels of peretinoin-response genes before treatment (No. 9–12) did not show HCC recurrence during the entire observation period (4.5 years; Table 1).

Hierarchical clustering of all 12 patients using 224 gene predictors is shown in Figure 2A. Clear gene clusters were observed according to patients with recurrence and those without, with the exception of one patient (No. 3, Table 1). Interestingly, in the liver of patients with non-recurrence, genes related to angiogenesis, cancer stem cells, Wnt signaling, and tumor progression were repressed, while genes inducing differentiation, tumor suppression, and apoptosis were up-regulated (Figure 2B, Table 4). Interestingly, PDGF-C was the most significant predictor to differentiate patients who will experience recurrence within 2 years (Table 4).

Consistent with these results, hierarchical clustering using pre-defined curated gene sets based on the NCBI's Cancer Genome Anatomy Project similarly differentiated patients into two groups with or without HCC recurrence (Figure 3). Among angiogenesis-related genes, PDGF-C, PDGF-B, vascular endothelial growth factor (VEGF)-B, VEGF-D, and fibroblast growth factor-basic (FGF-2) were repressed in patients without recurrence. As for cell signaling-related genes, MYC, SRC, and RAS-related genes were also repressed; retinoid X receptor alpha (RXRA) and CCAAT/enhancer binding protein (C/EBP), alpha were up-regulated in patients without recurrence. Some cytokines (IL-7, IL-13, and IL-18) and chemokines (e.g. CXCL7) were repressed, while major histocompatibility complex molecules and interferon-related molecules (e.g. IFNAR2) were up-regulated in patients without recurrence (Figure 3).

cDNA microarray analysis revealed that among these predictors, the mRNA level of PDGF-C was the most significant predictor for differentiating patients who will experience recurrence within 2 years (Table 4). This observation was also assessed by RTD-PCR (Figure 4). The expression of the catalytic enzyme of retinoic acid, CYP26B1, was significantly up-regulated at around 200 fold by peretinoin treatment, but its expression was equally induced in patients with or without recurrence. However, the expression of RAR-β, a retinoid receptor, was significantly up-regulated by peretinoin in patients without HCC recurrence (Figure 4).

Patients were followed up for a further 3 years (mean: 2.5 ± 0.5 years) after the cessation of peretinoin treatment. Other two patients experienced recurrence during

Table 2 Representative genes significantly up-regulated or down-regulated in response to peretinoin treatment

Parametric p-value	Ratios (Under/Pre)		Description	Symbol	GB acc
600 mg	600 mg	300 mg			
Up-regulated genes in response to peretinoin treatment					
Retinoid target genes					
0.0002	1.85	1.25	Cytochrome P450, family 26, subfamily B, polypeptide 1	CYP26B1	NM_019885
0.004	1.75	1.33	Insulin-like growth factor binding protein 6	IGFBP6	NM_002178
0.005	1.42	1.16	Regulatory factor X-associated ankyrin-containing protein	RFXANK	NM_134440
0.006	1.33	1.30	Putative lymphocyte G0/G1 switch gene	G0S2	NM_015714
0.013	1.54	0.90	Retinol binding protein 1	RBP1	NM_002899
0.014	1.56	0.87	Retinol binding protein 4	RBP4	NM_006744
0.034	1.27	1.07	Retinoic acid induced 3	GPRC5A	AI923823
0.040	1.22	1.19	Transglutaminase 2	TGM2	AI962033
0.044	1.23	1.14	CCAAT/enhancer binding protein (C/EBP), alpha	CEBPA	NM_004364
Interferon-related genes					
0.029	1.45	0.93	Guanylate binding protein 1, interferon-inducible, 67kDa	GBP1	NM_002053
0.047	1.39	0.94	Interferon-induced protein 44	IFI44	NM_006417
0.048	1.28	1.05	Chemokine (C-X-C motif) ligand 9	CXCL9	NM_002416
Negative regulator of Wnt and TGF-β signaling					
0.004	1.54	1.06	BMP and activin membrane-bound inhibitor homolog	BAMBI	NM_012342
0.008	1.45	1.11	Secreted frizzled-related protein 5	SFRP5	NM_003015
Anti-angiogenesis					
0.021	1.37	0.98	Thrombomodulin	THBD	NM_000361
0.038	1.28	0.99	Protein C receptor, endothelial (EPCR)	PROCR	NM_006404
Tumor suppressor related					
0.029	1.35	0.96	Jumonji domain containing 3	JMJD3	XM_043272
0.029	1.39	0.91	Jumping translocation breakpoint	JTB	NM_006694
0.034	1.39	1.32	Protein kinase, AMP-activated, alpha 2 catalytic subunit	PRKAA2	NM_006252
Down-regurated genes in response to peretinoin treatment					
mTOR-related-gene					
0.045	0.78	0.94	FK506 binding protein 12-rapamycin associated protein 1	FRAP1	NM_004958
Cytokine and growth factor					
0.019	0.77	1.25	Interleukin 13	IL13	NM_002188
0.031	0.74	1.00	Hepatocyte growth factor	HGF	NM_000601
Tumor progression related					
0.011	0.73	0.94	Junctional adhesion molecule 3	JAM3	NM_032801
0.013	0.70	1.00	V-myc myelocytomatosis viral oncogene homolog	Myc	NM_002467
0.017	0.73	1.12	Src-like-adaptor	SLA	NM_006748
0.028	0.78	1.10	Cell division cycle 2, G1 to S and G2 to M	CDC2	NM_001786
0.030	0.66	0.95	BCL2-associated athanogene	BAG1	NM_004323
0.039	0.64	0.93	Chemokine (C-C motif) receptor 9	CCR9	NM_031200
0.043	0.76	1.13	Pre-B-cell leukemia transcription factor 1	PBX1	H08835

The peretinoin-response genes were identified by comparing hepatic gene expression in the pre and under treatment of 6 patients who were treated with 600 mg dose of peretinoin. The fold changes of gene expression are shown in 300 mg and 600 mg dosage respectively.

Table 3 Supervised learning methods

Class		No. of predictors (p<0.002)	Prediction (%)	p-value
Pre-treatment	Recurrence vs non-recurrence	6	47.1	N.S.
On-treatment	Recurrence vs non-recurrence	224	79.6	< 0.05
On-treatment	300 mg vs 600 mg	38	72.7	N.S.

Seven algorithms of Compound-Covariate Predictor, Diagonal Linear Discriminant Analysis 1-Nearest Neighbor, 3-Nearest Neighbors, Nearest Centroid, Support Vector Machine, and Bayesian Compound Covariate were used for class prediction. Prediction % was calculated as the average of these seven algorithms.

further follow up period (No. 4 and No. 8 in Figure 2A, Table 1). Three patients with recurrence died at 0.3, 1.9, and 2.5 years after the cessation of peretinoin treatment. The Kaplan-Meier estimation of the recurrence-free ratio deduced from 224 gene predictors showed significant differences in HCC recurrence between patients with the recurrence expression pattern and those with non-recurrence expression (P=0.04). Moreover, Kaplan-Meier estimation of the survival ratio deduced from the same gene predictors showed a trend for improved survival of patients with non-recurrence expression patterns compared with those with the recurrence expression pattern (P=0.12) (Figure 2C, D).

With the exception of the number of tumors at the time of curative therapy, none of the other clinical parameters (e.g. peretinoin dose, tumor, background liver histology, or background liver function) were associated with the recurrence-free or survival ratio. Thus, the peretinoin response during the early period of administration deduced from the hepatic gene expression pattern can successfully predict HCC recurrence and, potentially, patient survival.

Discussion

Peretinoin [(2E,4E,6E,10E)-3,7,11,15-tetramethylhexadeca-2,4,6,10,14-pentaenoic acid] is expected to be a powerful agent against HCC recurrence. This synthetic retinoid induces the transcriptional activation of the retinoic acid receptor (RAR) and retinoid X receptor (RXR), which are both members of the retinoid receptor family. One primary pathway of HCC development involves sustained hepatitis virus infection, which causes repeated cycles of hepatocellular necrosis and proliferation. During increased cell proliferation, mutations occur that lead to the development of HCC unless the dedifferentiated tumor cells are eliminated by apoptosis. The anti-HCC mechanism of action of peretinoin has previously been suggested to be a result of induction of cell apoptosis [20,21], enhancement of cell differentiation [21,22], suppression of cell proliferation by elevation of P21 protein expression and suppression of cyclin D1 expression [23,24]. The first route of action is independent of retinoid receptors, while the others are retinoid receptor-dependent, although all mechanisms remain largely speculative.

Peretinoin was previously shown to suppress *in vivo* hepatocarcinogenesis in 3′-methyl-4-dimethylaminoazobenzene- and *N*-diethylnitrosamine-induced rats [14,15,25], and in hepatoma-bearing mice and transgenic mice expressing a dominant-negative retinoic acid receptor [25,26]. Recently, we revealed that peretinoin effectively inhibits hepatic fibrosis and HCC development in *Pdgf-c Tg* mice. This demonstrated that PDGF signaling is a target of peretinoin in preventing the development of hepatic fibrosis and HCC [27]. The purpose of this study was to investigate how peretinoin exerts its therapeutic potential by analyzing its effects on the gene expression patterns in clinical samples.

Gene expression profiling in patients without HCC recurrence demonstrated the promotion of *RAR-β* expression, the most common retinoid target gene identified by basic research. Moreover, the expression of other retinoid target genes such as *C/EBP-α*, *IGFBP6*, *TGM2*, *G0S2*, *RBP1*, *RBP4*, and *GPRC5A* was also enhanced. Of these, *C/EBP-α*, *IGFBP6*, and *TGM2* have been shown to inhibit HCC proliferation when co-expressed with *RAR-β* by all-trans-retinoic acid [28,29]. In addition, the RXR-selective agonist (rexinoid)-induced expression of *IGFBP6*, which occurs following *RAR-β*-mediated transcriptional activation of *RAR/RXR*, has been shown to suppress tumor growth [30]. Moreover, *G0S2* and *GPRC5A* have been reported to possess tumor suppressive or apoptosis-inducing effects [31,32]. These primary response retinoid target genes are presumably retinoid-responsive genes. In addition to enhancing retinoid target gene expression, peretinoin induced changes in the expression levels of a variety of genes involved in hepatocarcinogenesis, such as those related to Wnt signaling, IGF signaling, interferon, mTOR, and cell cycle regulation. These results suggest that peretinoin modulates multiple signaling cascades involved in carcinogenesis, either directly or indirectly. Abnormalities in the genes regulating Wnt signaling, IGF signaling, interferon, mTOR, and the cell cycle have been indicated to play a crucial role in the development of HCC [33,34]. We argue that peretinoin suppresses HCC cell proliferation by improving the expression of these genes, thereby preventing HCC recurrence.

The cluster analysis performed in this study successfully differentiated patients with recurrence within 2 years and those without it. Supervised learning methods identified 224 genes as predictors for HCC recurrence (p<0.002). Importantly, 44 (20%) of these were peretinoin-responsive genes, suggesting that recurrence-related genes might be regulated by peretinoin-responsive genes.

A comparison of these groups of patients revealed that the non-recurrence group was associated with the

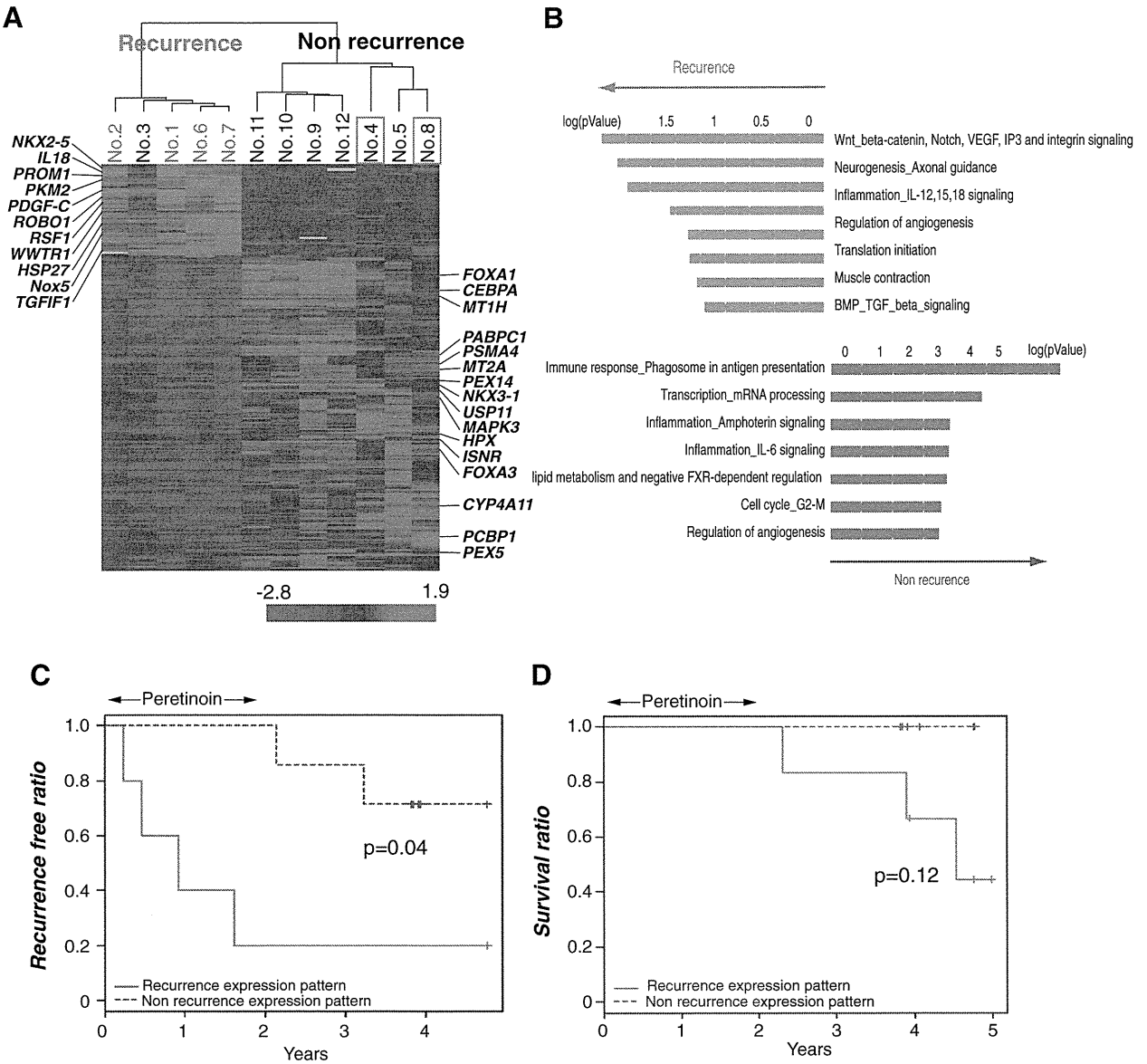

Figure 2 Expression profiling of 224 gene predictors and the prognosis of patients. A: Hierarchical clustering using 224 gene predictors of patients with or without HCC recurrence. Patients with HCC recurrence within 2 years are shown in red and patients with HCC recurrence after the cessation of peretinoin are boxed in red. **B**: Pathway analysis of differentially expressed genes using MetaCore (GeneGo). Functional ontology enrichment analysis was performed to find differentially expressed pathway maps or map folders using 224 differentially expressed genes ($p<0.002$) between patients with and without HCC recurrence. **C**, **D**: Kaplan-Meier estimation of recurrence-free ratio (**C**) and survival ratio (**D**) of patients with recurrence expression patterns (red) and those with non-recurrence expression (blue).

enhanced expression of genes related to hepatocellular differentiation and tumor suppression. The non-recurrence group also showed reduced expression of the genes promoting liver fibrosis and steatosis and the liver cancer stem cell marker genes. The genes related to hepatocellular differentiation, *MT1H*, *MT2A*, *FOXA1* (*HNF3α*), and *FOXA3* (*HNF3γ*), may be secondary response genes regulated by *C/EBP-α* [35,36]. Indeed, *C/EBP-α* manifested a significant shift in expression level before and during treatment with peretinoin, and could also differentiate between recurrence and non-recurrence within 2 years. Even after the cessation of peretinoin treatment, the expression of these genes was still significantly related to HCC recurrence (Figure 2C, D). Thus, we speculate that the differences in expression levels of peretinoin-response genes would determine the expression of recurrence-related genes (Additional file 3: Figure S2).

Interestingly, PDGF-C was the most significant predictor to differentiate those patients who will experience recurrence. Using a mouse model of PDGF-C over-

Table 4 Representative genes differentially expressed between HCC recurrence and non-recurrence groups

Parametric p-value	t-values	Description	Symbol	GB acc
Up-regulated genes in the recurrence group				
Angiogenesis related				
0.0001	−5.19	Platelet derived growth factor C	PDGFC	AI446155
0.0006	−4.37	Sperm equatorial segment protein 1	NOX5	NM_145658
0.0010	−4.13	Interleukin 18	IL18	AI800476
Cancer stem cell related				
0.0004	−4.63	Prominin 1	PROM1	NM_006017
0.0018	−3.83	Pyruvate kinase, muscle	PKM2	NM_002654
Positive regulator of Wnt				
0.0018	−3.84	TGFB-induced factor (TALE family homeobox)	TGIF1	AI866302
0.0018	−3.84	NK2 transcription factor related, locus 5	NKX2-5	NM_004387
Tumor progression related				
0.0005	−4.47	Transcriptional co-activator with PDZ-binding motif	WWTR1	AK025216
0.0017	−3.87	Roundabout, axon guidance receptor, homolog 1	ROBO1	NM_133631
0.0018	−3.84	Hepatitis B virus x associated protein	RSF1	NM_016578
0.0019	−3.79	Heat shock 27kDa protein 2	HSPB2	NM_001541
Up-regulated genes in the non-recurrence group				
Liver function and hepatocytes differenti related				
0.0002	4.88	Metallothionein 2A	MT2A	NM_005953
0.0002	4.08	CCAAT/enhancer binding protein (C/EBP), alpha	CEBPA	NM_004364
0.0003	4.72	Forkhead box A3	FOXA3	NM_004497
0.0006	4.42	Hemopexin	HPX	NM_000613
0.0006	4.35	Metallothionein 1H	MT1H	NM_005951
0.0013	4.01	Forkhead box A1	FOXA1	NM_004496
0.0014	3.97	FK506 binding protein 8, 38kDa	FKBP8	NM_012181
Tumor suppressor related				
0.0005	4.51	Deleted in colorectal carcinoma	DCC	X76132
0.0018	3.84	NK3 transcription factor related, locus 1	NKX3-1	NM_006167
Apoptosis inducing				
0.0015	3.93	BH3 interacting domain death agonist	BID	NM_197967
0.0019	3.82	Programmed cell death 8	AIFM1	NM_145813

expression resulting in hepatic fibrosis, steatosis, and eventually HCC development, peretinoin was previously shown to significantly repress the development of hepatic fibrosis and tumors [27].

Although gene expression profiling analysis was conducted using the remnant liver after definitive treatment in the present study, past similar research has demonstrated the possibility of predicting recurrent metachronous and multicentric HCC [37,38]. The exact mechanisms of how the expression profile of non-tumor tissues might determine the recurrence risk are not known. However, the degree of differentiation of hepatocytes and microenvironments such as angiogenesis and fibrogenesis in non-tumor lesions of the liver is likely to be closely associated with hepatocarcinogenesis. Interestingly, patients with pre-activated peretinoin-response genes were resistant to HCC recurrence for the entire observation period (4.5 years).

This study demonstrated that the patient response to peretinoin during the early period of administration could predict HCC recurrence and, potentially, patient survival. However, it should be noted that the current study protocol consisted of 600 mg peretinoin as the subsequent maintenance treatment for all patients after the 8-week start phase (Figure 1A). In addition, we did not conduct a placebo control to observe serial changes

Figure 3 Hierarchical clustering using pre-defined curated gene sets based on NCBI's Cancer Genome Anatomy Project. Presented genes were differentially expressed at *P*-values <0.05 between patients with and without HCC recurrence.

of hepatic gene expression without peretinoin administration. Therefore, there might be some limitations in drawing concrete conclusions from this study.

Although we attempted to analyze the liver peretinoin concentration in the present study to investigate its possible relationship with gene expression, peretinoin levels were too low to yield a meaningful result. However, considering that gene expression profiling identified significant changes in the expression levels of retinoid-related and other genes before and during peretinoin treatment, we believe that sufficient levels of peretinoin reached the liver.

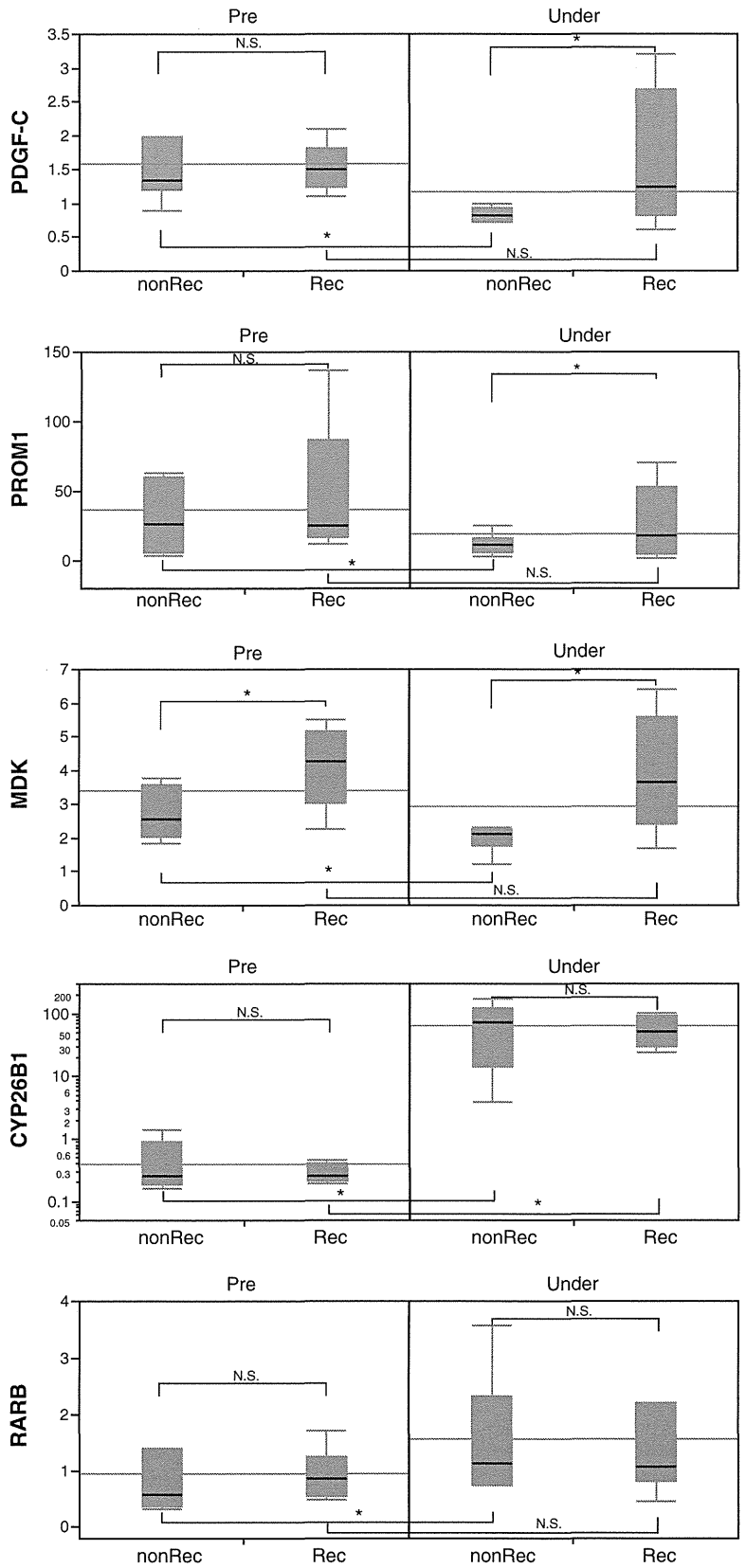

Figure 4 RTD-PCR evaluation of PDGF-C, PROM1, MDK, CYP26B1, and RAR β in the liver of patients with or without HCC recurrence.

The previous peretinoin phase II/III clinical study demonstrated that daily doses of 600 mg peretinoin significantly reduced the incidence of HCC recurrence in HCV-positive patients who underwent definitive treatment. The findings of the present study are complementary to this as we successfully identified candidates for the peretinoin-responsive and recurrence-related genes. These genes are probably involved in the inhibition of HCC recurrence and could be beneficial as future candidate biomarkers of the effectiveness of peretinoin.

Conclusions

In this study, patients underwent liver biopsy before and after 8 weeks of treatment with repeated doses of peretinoin. Gene expression profiling at week 8 of peretinoin treatment could successfully predict HCC recurrence within 2 years. This study is the first to show the effect of peretinoin in suppressing HCC recurrence *in vivo* based on gene expression profiles and provides a molecular basis for understanding the efficacy of peretinoin.

Additional files

Additional file 1: Study protocol.

Additional file 2: Figure S1. One-way hierarchical clustering of up-regulated or down-regulated genes in the liver by the administration of peretinoin (300 mg and 600 mg). Changes in gene expression in the liver before the start of peretinoin administration and 8 weeks into the treatment are shown. Patients with HCC recurrence within 2 years are shown in red and those with HCC recurrence after the cessation of peretinoin are boxed in red.

Additional file 3: Figure S2. Schematic representation of peretinoin action in the liver.

Abbreviations

ACR: Acyclic Retinoid; CH-C: Chronic Hepatitis C; HCC: Hepatocellular Carcinoma; HCV: Hepatitis C Virus.

Competing interests

The authors declare that they have no competing interests.

Authors' contributions

MH: study concept and design, manuscript preparation. TY: gene expression analysis. TY: acquisition of data of clinical data. KA: acquisition of data of clinical data. YS: gene expression analysis. AS: acquisition of data of clinical data. MN: gene expression analysis. EM: acquisition of data of clinical. SK: study concept and design. All authors read and approved the final manuscript.

Acknowledgements

The authors thank Nami Nishiyama for excellent technical assistance.
This work was supported in part by KOWA Co. Ltd., Tokyo, Japan.

Received: 13 September 2012 Accepted: 8 March 2013
Published: 15 April 2013

References

1. Ferlay J, Shin HR, Bray F, Forman D, Mathers C, Parkin DM: **Estimates of worldwide burden of cancer in 2008: GLOBOCAN 2008.** *Int J Cancer* 2010, **127**(12):2893–2917.
2. Altekruse SF, McGlynn KA, Reichman ME: **Hepatocellular carcinoma incidence, mortality, and survival trends in the United States from 1975 to 2005.** *J Clin Oncol* 2009, **27**(9):1485–1491.
3. Llovet JM, Burroughs A, Bruix J: **Hepatocellular carcinoma.** *Lancet* 2003, **362**(9399):1907–1917.
4. Llovet JM, Bru C, Bruix J: **Prognosis of hepatocellular carcinoma: the BCLC staging classification.** *Semin Liver Dis* 1999, **19**(3):329–338.
5. Mazzaferro V, Regalia E, Doci R, Andreola S, Pulvirenti A, Bozzetti F, Montalto F, Ammatuna M, Morabito A, Gennari L: **Liver transplantation for the treatment of small hepatocellular carcinomas in patients with cirrhosis.** *N Engl J Med* 1996, **334**(11):693–699.
6. Llovet JM, Schwartz M, Mazzaferro V: **Resection and liver transplantation for hepatocellular carcinoma.** *Semin Liver Dis* 2005, **25**(2):181–200.
7. Castells A, Bruix J, Bru C, Fuster J, Vilana R, Navasa M, Ayuso C, Boix L, Visa J, Rodes J: **Treatment of small hepatocellular carcinoma in cirrhotic patients: a cohort study comparing surgical resection and percutaneous ethanol injection.** *Hepatology* 1993, **18**(5):1121–1126.
8. Shiratori Y, Shiina S, Teratani T, Imamura M, Obi S, Sato S, Koike Y, Yoshida H, Omata M: **Interferon therapy after tumor ablation improves prognosis in patients with hepatocellular carcinoma associated with hepatitis C virus.** *Ann Intern Med* 2003, **138**(4):299–306.
9. Breitenstein S, Dimitroulis D, Petrowsky H, Puhan MA, Mullhaupt B, Clavien PA: **Systematic review and meta-analysis of interferon after curative treatment of hepatocellular carcinoma in patients with viral hepatitis.** *Br J Surg* 2009, **96**(9):975–981.
10. Samuel M, Chow PK, Chan Shih-Yen E, Machin D, Soo KC: **Neoadjuvant and adjuvant therapy for surgical resection of hepatocellular carcinoma.** *Cochrane Database Syst Rev* 2009, **1**:CD001199.
11. Mathurin P, Raynard B, Dharancy S, Kirzin S, Fallik D, Pruvot FR, Roumilhac D, Canva V, Paris JC, Chaput JC, *et al*: **Meta-analysis: evaluation of adjuvant therapy after curative liver resection for hepatocellular carcinoma.** *Aliment Pharmacol Ther* 2003, **17**(10):1247–1261.
12. Muto Y, Moriwaki H, Ninomiya M, Adachi S, Saito A, Takasaki KT, Tanaka T, Tsurumi K, Okuno M, Tomita E, *et al*: **Prevention of second primary tumors by an acyclic retinoid, polyprenoic acid, in patients with hepatocellular carcinoma. Hepatoma Prevention Study Group.** *N Engl J Med* 1996, **334**(24):1561–1567.
13. Muto Y, Moriwaki H, Saito A: **Prevention of second primary tumors by an acyclic retinoid in patients with hepatocellular carcinoma.** *N Engl J Med* 1999, **340**(13):1046–1047.
14. Sano T, Kagawa M, Okuno M, Ishibashi N, Hashimoto M, Yamamoto M, Suzuki R, Kohno H, Matsushima-Nishiwaki R, Takano Y, *et al*: **Prevention of rat hepatocarcinogenesis by acyclic retinoid is accompanied by reduction in emergence of both TGF-alpha-expressing oval-like cells and activated hepatic stellate cells.** *Nutr Cancer* 2005, **51**(2):197–206.
15. Kagawa M, Sano T, Ishibashi N, Hashimoto M, Okuno M, Moriwaki H, Suzuki R, Kohno H, Tanaka T: **An acyclic retinoid, NIK-333, inhibits N-diethylnitrosamin-einduced rat hepatocarcinogenesis through suppression of TGF-alpha expression and cell proliferation.** *Carcinogenesis* 2004, **25**(6):979–985.
16. Okusaka T, Ueno H, Ikeda M, Morizane C: **Phase I and pharmacokinetic clinical trial of oral administration of the acyclic retinoid NIK-333.** *Hepatol Res* 2011, **41**(6):542–552.
17. Okita K, Matsui O, Kumada H, Tanaka K, Kaneko S, Moriwaki H, Izumi N, Okusaka T, Ohashi Y, Makuuchi M: **Effect of peretinoin on recurrence of hepatocellular carcinoma (HCC): Results of a phase II/III randomized placebo-controlled trial.** *J Clin Oncol* 2010, **15s**(28Suppl):4024.
18. Honda M, Yamashita T, Ueda T, Takatori H, Nishino R, Kaneko S: **Different signaling pathways in the livers of patients with chronic hepatitis B or chronic hepatitis C.** *Hepatology* 2006, **44**(5):1122–1138.
19. Honda M, Sakai A, Yamashita T, Nakamoto Y, Mizukoshi E, Sakai Y, Yamashita T, Nakamura M, Shirasaki T, Horimoto K, *et al*: **Hepatic ISG expression is associated with genetic variation in interleukin 28B and the outcome of IFN therapy for chronic hepatitis C.** *Gastroenterology* 2010, **139**(2):499–509.
20. Nakamura N, Shidoji Y, Yamada Y, Hatakeyama H, Moriwaki H, Muto Y: **Induction of apoptosis by acyclic retinoid in the human hepatoma-derived cell line, HuH-7.** *Biochem Biophys Res Commun* 1995, **207**(1):382–388.
21. Yasuda I, Shiratori Y, Adachi S, Obora A, Takemura M, Okuno M, Shidoji Y, Seishima M, Muto Y, Moriwaki H: **Acyclic retinoid induces partial differentiation, down-regulates telomerase reverse transcriptase mRNA**

expression and telomerase activity, and induces apoptosis in human hepatoma-derived cell lines. *J Hepatol* 2002, **36**(5):660–671.
22. Yamada Y, Shidoji Y, Fukutomi Y, Ishikawa T, Kaneko T, Nakagama H, Imawari M, Moriwaki H, Muto Y: **Positive and negative regulations of albumin gene expression by retinoids in human hepatoma cell lines.** *Mol Carcinog* 1994, **10**(3):151–158.
23. Suzui M, Masuda M, Lim JT, Albanese C, Pestell RG, Weinstein IB: **Growth inhibition of human hepatoma cells by acyclic retinoid is associated with induction of p21(CIP1) and inhibition of expression of cyclin D1.** *Cancer Res* 2002, **62**(14):3997–4006.
24. Suzui M, Shimizu M, Masuda M, Lim JT, Yoshimi N, Weinstein IB: **Acyclic retinoid activates retinoic acid receptor beta and induces transcriptional activation of p21(CIP1) in HepG2 human hepatoma cells.** *Mol Cancer Ther* 2004, **3**(3):309–316.
25. Muto Y, Moriwaki H: **Antitumor activity of vitamin A and its derivatives.** *J Natl Cancer Inst* 1984, **73**(6):1389–1393.
26. Sakabe T, Tsuchiya H, Endo M, Tomita A, Ishii K, Gonda K, Murai R, Takubo K, Hoshikawa Y, Kurimasa A, *et al*: **An antioxidant effect by acyclic retinoid suppresses liver tumor in mice.** *Biochem Pharmacol* 2007, **73**(9):1405–1411.
27. Okada H, Honda M, Campbell JS, Sakai Y, Yamashita T, Takebuchi Y, Hada K, Shirasaki T, Takabatake R, Nakamura M, *et al*: **Acyclic retinoid targets platelet-derived growth factor signaling in the prevention of hepatic fibrosis and hepatocellular carcinoma development.** *Cancer Res* 2012, **72**(17):4459–4471.
28. Tomaru Y, Nakanishi M, Miura H, Kimura Y, Ohkawa H, Ohta Y, Hayashizaki Y, Suzuki M: **Identification of an inter-transcription factor regulatory network in human hepatoma cells by Matrix RNAi.** *Nucleic Acids Res* 2009, **37**(4):1049–1060.
29. Nakanishi M, Tomaru Y, Miura H, Hayashizaki Y, Suzuki M: **Identification of transcriptional regulatory cascades in retinoic acid-induced growth arrest of HepG2 cells.** *Nucleic Acids Res* 2008, **36**(10):3443–3454.
30. Uray IP, Shen Q, Seo HS, Kim H, Lamph WW, Bissonnette RP, Brown PH: **Rexinoid-induced expression of IGFBP-6 requires RARbeta-dependent permissive cooperation of retinoid receptors and AP-1.** *J Biol Chem* 2009, **284**(1):345–353.
31. Ma Y, Koza-Taylor PH, DiMattia DA, Hames L, Fu H, Dragnev KH, Turi T, Beebe JS, Freemantle SJ, Dmitrovsky E: **Microarray analysis uncovers retinoid targets in human bronchial epithelial cells.** *Oncogene* 2003, **22**(31):4924–4932.
32. Ye X, Tao Q, Wang Y, Cheng Y, Lotan R: **Mechanisms underlying the induction of the putative human tumor suppressor GPRC5A by retinoic acid.** *Cancer Biol Ther* 2009, **8**(10):951–962.
33. Llovet JM, Bruix J: **Molecular targeted therapies in hepatocellular carcinoma.** *Hepatology* 2008, **48**(4):1312–1327.
34. Zender L, Villanueva A, Tovar V, Sia D, Chiang DY, Llovet JM: **Cancer gene discovery in hepatocellular carcinoma.** *J Hepatol* 2010, **52**(6):921–929.
35. Datta J, Majumder S, Kutay H, Motiwala T, Frankel W, Costa R, Cha HC, MacDougald OA, Jacob ST, Ghoshal K: **Metallothionein expression is suppressed in primary human hepatocellular carcinomas and is mediated through inactivation of CCAAT/enhancer binding protein alpha by phosphatidylinositol 3-kinase signaling cascade.** *Cancer Res* 2007, **67**(6):2736–2746.
36. Fields AL, Soprano DR, Soprano KJ: **Retinoids in biological control and cancer.** *J Cell Biochem* 2007, **102**(4):886–898.
37. Hoshida Y, Villanueva A, Kobayashi M, Peix J, Chiang DY, Camargo A, Gupta S, Moore J, Wrobel MJ, Lerner J, *et al*: **Gene expression in fixed tissues and outcome in hepatocellular carcinoma.** *N Engl J Med* 2008, **359**(19):1995–2004.
38. Utsunomiya T, Shimada M, Imura S, Morine Y, Ikemoto T, Mori M: **Molecular signatures of noncancerous liver tissue can predict the risk for late recurrence of hepatocellular carcinoma.** *J Gastroenterol* 2010, **45**(2):146–152.

doi:10.1186/1471-2407-13-191
Cite this article as: Honda *et al.*: Peretinoin, an acyclic retinoid, improves the hepatic gene signature of chronic hepatitis C following curative therapy of hepatocellular carcinoma. *BMC Cancer* 2013 13:191.

THE JOURNAL OF BIOLOGICAL CHEMISTRY VOL. 289, NO. 1, pp. 335–345, January 3, 2014

Metformin Suppresses Expression of the Selenoprotein P Gene via an AMP-activated Kinase (AMPK)/FoxO3a Pathway in H4IIEC3 Hepatocytes*[S]

Received for publication, May 1, 2013, and in revised form, November 18, 2013 Published, JBC Papers in Press, November 20, 2013, DOI 10.1074/jbc.M113.479386

Hiroaki Takayama,[a] Hirofumi Misu,[a] Hisakazu Iwama,[b] Keita Chikamoto,[a,c] Yoshiro Saito,[d] Koji Murao,[e] Atsushi Teraguchi,[f] Fei Lan,[a] Akihiro Kikuchi,[a] Reina Saito,[a] Natsumi Tajima,[a] Takayoshi Shirasaki,[a,g] Seiichi Matsugo,[h,i] Ken-ichi Miyamoto,[j,k] Shuichi Kaneko,[a] and Toshinari Takamura[a1]

From the [a]Department of Disease Control and Homeostasis, Kanazawa University Graduate School of Medical Sciences, 13-1 Takara-machi, Kanazawa, Ishikawa 920-8641, Japan, the [b]Life Science Research Center, Kagawa University, Ikenobe 1750-1, Miki-cho, Kita-gun, Kagawa 761-0793, Japan, the [c]Division of Natural System, Graduate School of Natural Science and Technology, Kanazawa University, Kakuma-machi, Kanazawa, Ishikawa 920-1192, Japan, the [d]Systems Life Sciences, Department of Medical Life Systems, Faculty of Medical and Life Sciences, Doshisha University, Kyotanabe, Kyoto 610-0394, Japan, the [e]Departments of Advanced Medicine, Kagawa University, Ikenobe 1750-1, Miki-cho, Kita-gun, Kagawa 761-0793, Japan, the [f]Department of Hospital Pharmacy, Kanazawa University, 13-1 Takara-machi, Kanazawa, Ishikawa 920-8641, Japan, the [g]Department of Advanced Medical Technology, Kanazawa University Graduate School of Health Medicine, 13-1 Takara-machi, Kanazawa, Ishikawa 920-8641, Japan, the [h]Division of Material Engineering, Graduate School of Natural Science and Technology, Kanazawa University, Kakuma-machi, Kanazawa, Ishikawa 920-1192, Japan, the [i]Institute of Science and Engineering, Faculty of Natural System, Kanazawa University, Kakuma-machi, Kanazawa, Ishikawa 920-1192, Japan, the [j]Department of Hospital Pharmacy, Kanazawa University Graduate School of Medical Sciences, 13-1 Takara-machi, Kanazawa, Ishikawa 920-8641, Japan, and the [k]Department of Medicinal Informatics, Kanazawa University Graduate School of Medical Sciences, 13-1 Takara-machi, Kanazawa, Ishikawa 920-8641, Japan

Background: The suppression of selenoprotein P production may be a novel therapeutic target for reducing insulin resistance.
Results: Selenoprotein P expression was suppressed by metformin treatment, but co-administration of AMPK inhibitor or FoxO3a siRNA cancelled this suppression.
Conclusion: Metformin suppresses selenoprotein P expression via the AMPK/FoxO3a pathway.
Significance: The AMPK/FoxO3a pathway in the liver may be a therapeutic target for type 2 diabetes.

Selenoprotein P (SeP; encoded by *SEPP1* in humans) is a liver-derived secretory protein that induces insulin resistance in type 2 diabetes. Suppression of SeP might provide a novel therapeutic approach to treating type 2 diabetes, but few drugs that inhibit *SEPP1* expression in hepatocytes have been identified to date. The present findings demonstrate that metformin suppresses *SEPP1* expression by activating AMP-activated kinase (AMPK) and subsequently inactivating FoxO3a in H4IIEC3 hepatocytes. Treatment with metformin reduced *SEPP1* promoter activity in a concentration- and time-dependent manner; this effect was cancelled by co-administration of an AMPK inhibitor. Metformin also suppressed *Sepp1* gene expression in the liver of mice. Computational analysis of transcription factor binding sites conserved among the species resulted in identification of the FoxO-binding site in the metformin-response element of the *SEPP1* promoter. A luciferase reporter assay showed that metformin suppresses Forkhead-response element activity, and a ChIP assay revealed that metformin decreases binding of FoxO3a, a direct target of AMPK, to the *SEPP1* promoter. Transfection with siRNAs for *Foxo3a*, but not for *Foxo1*, cancelled metformin-induced luciferase activity suppression of the metformin-response element of the *SEPP1* promoter. The overexpression of FoxO3a stimulated *SEPP1* promoter activity and rescued the suppressive effect of metformin. Metformin did not affect FoxO3a expression, but it increased its phosphorylation and decreased its nuclear localization. These data provide a novel mechanism of action for metformin involving improvement of systemic insulin sensitivity through the regulation of SeP production and suggest an additional approach to the development of anti-diabetic drugs.

Selenoprotein P (SeP[2]; encoded by *SEPP1* in humans) is a secretory protein produced mainly by the liver (1, 2). SeP contains 10 selenocysteine residues and is known to transport the essential trace element selenium from the liver to the rest of the

* This work was supported by grants-in-aid from the Ministry of Education, Culture, Sports, Science and Technology, Japan (to H. M., T. T., and S. K.) and research grants from Dainippon Sumitomo Pharma (to S. K.) and Takeda Science Foundation (to H. M.).
[S] This article contains supplemental Figs. S1–S5.
[1] To whom correspondence should be addressed: Dept. of Disease Control and Homeostasis, Kanazawa University Graduate School of Medical Science, 13-1 Takara-machi, Kanazawa, Ishikawa 920-8641, Japan. Tel.: 81-76-265-2233; Fax: 81-76-234-4250; E-mail: ttakamura@m-kanazawa.jp.

[2] The abbreviations used are: SeP, selenoprotein P; AMPK, AMP-activated kinase; AICAR, 5-aminoimidazole-4-carboxamide ribonucleotide; compound C, 6-[4-(2-piperidin-1-yl-ethoxy)-phenyl)]-3-pyridin-4-yl-pyrrazolo[1,5-a]-pyrimidine; cGPx, cellular glutathione peroxidase; DN, dominant negative; CA, constitutive active; TFBS, transcription factor binding site; FHRE, forkhead-response element.

body (3, 4). Our laboratory reported recently that SeP functions as a hepatokine that contributes to insulin resistance in type 2 diabetes (5). Using comprehensive gene expression analyses in humans, hepatic gene expression levels of *SEPP1* were found to be positively correlated with the severity of insulin resistance in patients with type 2 diabetes. Moreover, treatment with purified SeP protein impairs insulin signal transduction in both cell culture and animal models. Importantly, the RNA interference-mediated knockdown of SeP improves insulin resistance and hyperglycemia in a mouse model of type 2 diabetes, suggesting that the suppression of SeP production in the liver may be a novel therapeutic target for reducing insulin resistance in type 2 diabetes (5). However, few drugs that inhibit the production of SeP by hepatocytes have been identified to date.

Metformin is widely used as an anti-diabetic drug globally. The primary target of metformin action is the liver, which abundantly expresses organic cation transporter (Oct)-1, a transporter for metformin (6, 7). Adenosine monophosphate-activated protein kinase (AMPK) mediates primarily the glucose-lowering actions of metformin, including the suppression of hepatic gluconeogenesis (8). In contrast, several reports indicate that the oral administration of metformin in humans increases insulin sensitivity in skeletal muscle, increases serum adiponectin, and improves aortic arteriosclerosis (9–11). These reports suggest that orally administered metformin also exerts beneficial actions on tissues other than the liver, in which expression levels of Octs are lower. To date, however, the molecular mechanisms underlying the systemic actions of metformin are not fully understood.

Forkhead box protein O3a (FoxO3a), which belongs to the Forkhead transcription factors of the FoxO subfamily (FoxOs), is reported to be involved in cell cycle arrest (12), apoptosis (13), and the oxidative stress response (14, 15). Recently, Greer *et al.* (16) showed that FoxO3a, but not FoxO1, is directly phosphorylated and activated by AMPK *in vitro*. FoxO3a is reported to positively regulate mitochondria-related genes, such as uncoupling proteins, in mouse embryonic fibroblasts, suggesting that the direct regulation of FoxO3a by AMPK plays a crucial role in the control of the cellular energy balance. The phosphorylation of FoxO3a by AMPK was also identified in C2C12 myotubes (17), aortic vascular endothelial cells (18), and A549 lung cancer cells (19). However, the role of the AMPK/FoxO3a pathway in hepatocytes, an important target of metformin, remains unknown.

We demonstrate here that metformin suppresses *SEPP1* gene expression by activating AMPK and subsequently inactivating FoxO3a in H4IIEC3 hepatocytes. These results suggest a novel mechanism underlying the glucose-lowering action of metformin.

EXPERIMENTAL PROCEDURES

Materials—The antibodies against AMPKα, phospho-AMPKα, FoxO1, FoxO3a, acetylated Lys, and Lamin A/C were purchased from Cell Signaling Technology (Beverly, MA). Antibody against phospho-Ser/Thr/Tyr was purchased from AnaSpec (San Jose, CA). Antibody against GAPDH was purchased from Santa Cruz Biotechnology, Inc. 5-Aminoimidazole-4-carboxamide ribonucleotide (AICAR) and 6-[4-(2-Piperidin-1-yl-ethoxy)-phenyl)]-3-pyridin-4-yl-pyrrazolo [1,5-a]-pyrimidine (compound C) were purchased from Sigma-Aldrich. FoxO3a expression vector was provided from Ajinomoto Pharma (Tokyo, Japan) described before (20). Selenious acid was purchased from WaKo Pure Chemical Industries, Ltd. (Osaka, Japan). Metformin was provided by Dainippon Sumitomo Pharma (Osaka, Japan).

Generation of Plasmid Constructs—The human *SEPP1* promoter region has been described previously (21). Fragments of ~1800 bp from the human *SEPP1* promoter region and the deletion promoter region were amplified by PCR using normal human genomic DNA as a template and the primer pairs shown in Table 1. The PCR product was subcloned into the luciferase reporter gene plasmid pGL3-basic (Promega, Madison, WI) and termed "*SEPP1*-Promoter-Luc," "Mut-A," "Mut-B," "Mut-C," "Mut-D," "Mut-E," "Mut-DΔ1," "Mut-DΔ2," and "Mut-DΔ3." Putative FoxO binding site-deficient vector were generated using QuikChange Lightning site-directed mutagenesis kits (Agilent Technologies, Santa Clara, CA), according to the manufacturer's instructions. All inserts were confirmed by DNA sequencing.

Cell Culture—Studies were performed using the rat hepatoma cell line H4IIEC3 (American Type Culture Collection, Manassas, VA). Cells were cultured in Dulbecco's modified Eagle's medium (DMEM; Invitrogen) and supplemented with 10% fetal bovine serum (Invitrogen), 2 mmol/liter L-glutamine (WaKo Pure Chemical Industries, Ltd.), 100 units/ml penicillin, and 0.1 mg/ml streptomycin (WaKo Pure Chemical Industries, Ltd.). The cells were cultured at 37 °C in a humidified atmosphere containing 5% CO_2.

Measurement of Glutathione Peroxidase Activity—To measure cellular glutathione peroxidase (cGPx) activity, a coupled enzyme assay, which was performed by following the oxidation of NADPH, was used as described previously (22). In brief, cells were cultured with 1) DMEM plus 10% FBS, 2) DMEM plus 10% FBS and 100 nM selenious acid, or 3) DMEM plus 10% FBS and 1000 nM selenious acid at 72 h. Then cells were fractured with homogenate buffer containing 0.25 M sucrose, 50 mM Tris-HCl (pH 7.4), 0.1 mM EDTA, 0.1 mM 2-mercaptoethanol. The assay conditions were as follows for the cGPx assay: 0.1 M phosphate buffer, pH 7.4, 0.2 mM NADPH, 0.5 mM EDTA, 1 mM NaN_3, 2 mM GSH, 1 unit/ml GSH reductase, and 30 μM hydrogen peroxide. The oxidation of NADPH was followed at 340 nm at 37 °C, and units of the enzyme activity were expressed as μmol of NADPH oxidized/min.

Transfection and Luciferase Reporter Gene Assay—H4IIEC3 cells were grown in 24-well plates and transfected with 0.4 μg of plasmid DNA/well together with 1.2 μl of FuGENE6 (Promega). For the luciferase reporter gene assays, 0.4 μg of firefly luciferase promoter construct was co-transfected with 0.01 μg of *Renilla* luciferase control plasmid (pRL-SV40; Promega) and/or 0.05–0.4 μg of plasmids expressing FoxO3a or empty control plasmids, resulting in a total DNA amount of 0.41–0.81 μg/well. 24 h later, cells were treated with the indicated reagents, such as metformin, in DMEM plus 10% FBS for the indicated times. After 48 h, luciferase activities were measured using the Dual Luciferase assay system (Promega), as described previously (20).

TABLE 1
Primers used in cloning

Primer	Description	Sequence
SEPP1-Promoter-Luc		
Forward	hSeP-promoter-F-BglII	ACTAGATCTACAAACCTTTCAGACACTGAGTTG
Reverse	hSeP-promoter-R-NcoI	ACTCCATGGACAACCACTTCCAACGGGCCTGCTT
Mut-A		
Forward	hSeP-promoter-Del-F1-BglII	ACTAGATCTGGGCTGCCTGTCTTTGATTTCACAT
Reverse	hSeP-promoter-R-NcoI	ACTCCATGGACAACCACTTCCAACGGGCCTGCTT
Mut-B		
Forward	hSeP-promoter-Del-F2-BglII	ACTAGATCTTTGTAGTTCCTGCACCTTGTACAAC
Reverse	hSeP-promoter-R-NcoI	ACTCCATGGACAACCACTTCCAACGGGCCTGCTT
Mut-C		
Forward	hSeP-promoter-Del-F3-BglII	ACTAGATCTGCATAGGTCTTCCAGGAAGTACGAC
Reverse	hSeP-promoter-R-NcoI	ACTCCATGGACAACCACTTCCAACGGGCCTGCTT
Mut-D		
Forward	hSeP-promoter-Del-F4-BglII	ACTAGATCTCAAATGTTTTTCCCTGTTATAGTTT
Reverse	hSeP-promoter-R-NcoI	ACTCCATGGACAACCACTTCCAACGGGCCTGCTT
Mut-E		
Forward	hSeP-promoter-F-BglII	ACTAGATCTACAAACCTTTCAGACACTGAGTTG
Reverse	hSeP-promoter-Del-R1-NocI	ACTCCATGGCTGAGCCAGCGAATTATGCTGCTGC
Mut-DΔ1		
Forward	hSeP-promoter-Del-F14-BglII	ACTAGATCTGATTCTAGGGTGACTGAAAAGGATA
Reverse	hSeP-promoter-R-NcoI	ACTCCATGGACAACCACTTCCAACGGGCCTGCTT
Mut-DΔ2		
Forward	hSeP-promoter-Del-F15-BglII	ACTAGATCTATAACAATCAGCTCAGGGGTTTGCT
Reverse	hSeP-promoter-R-NcoI	ACTCCATGGACAACCACTTCCAACGGGCCTGCTT
Mut-DΔ3		
Forward	hSeP-promoter-Del-F16-BglII	ACTAGATCTATAAATATCAGAGTGTGCTGCTGTG
Reverse	hSeP-promoter-R-NcoI	ACTCCATGGACAACCACTTCCAACGGGCCTGCTT
Mut-DΔ2-ΔFoxo A		
Forward	del86–95	GACTATACCTGAGGGGTGAGGGACTATAAATATCAGAGTG
Reverse	del86–95-antisense	CACTCTGATATTTATAGTCCCTCACCCCTCAGGTATAGTC
Mut-DΔ2-ΔFoxo B		
Forward	hSeP-del-Foxo 3-F	GAGGTAAACAACAGGACTAAGAGTGTGCTGCTGTGG
Reverse	hSeP-del-Foxo 3-R	CCACAGCAGCACACTCTTAGTCCTGTTGTTTACCTC

siRNA Transfection in H4IIEC3 Hepatocytes—H4IIEC3 hepatocytes were grown in 24-well plates and transiently transfected with 10 nM small interfering RNA (siRNA) duplex oligonucleotides using 1 μl of Lipofectamine™ RNAiMAX (Invitrogen) by the reverse transfection method according to the manufacturer's instructions. *Foxo1*- and *Foxo3a*-specific siRNAs with the following sequences were synthesized (Thermo Scientific): *Foxo1* A, 5′-GACAGCAAAUCAAGUUAUG-3′ (sense); *Foxo1* B, 5′-UUUGAUAACUGGAGUACAU-3′ (sense); *Foxo3a* A, 5′-GAACGUUGUUGGUUUGAAC-3′ (sense); and *Foxo3a* B, 5′-CGUCAUGGGUCACGACAAG-3′ (sense). Negative control siRNA was also utilized (Thermo Scientific). 24 h after transfection, the cells were treated with metformin for 24 h, followed by the extraction of total RNA.

Adenovirus-mediated Gene Transfer in H4IIEC3 Hepatocytes—Cells were transfected with adenoviruses as described previously (5). Briefly, H4IIEC3 hepatocytes were grown to 90% confluence in 24-well multiplates and transfected with adenoviruses encoding dominant negative (DN) α1 and α2 AMPK, constitutive active (CA) AMPK, or LacZ for 4 h. The cells were incubated with DMEM for 24 h after removing the adenoviruses; total RNA was then extracted.

Quantitative RT-PCR—Total RNA was extracted from cultured H4IIEC3 hepatocytes using a Genelute mammalian total RNA miniprep kit (Sigma). The reverse transcription of 100 ng of total RNA was performed using a high capacity cDNA reverse transcription kit (Invitrogen), according to the manufacturer's instructions. Quantitative RT-PCR was performed using TaqMan probes (ACTB, 4352340E; Foxo1, Rn01494868_m1; Foxo3, Rn01441087_m1; G6pc, Rn00565347_m1; Pck1, Rn01529014_m1; Sepp1, Rn00569905_m1) and the 7900HT fast real-time PCR system (Invitrogen), as described previously (23).

Western Blotting—Treated cells were collected and lysed as described previously (20). Protein samples (10 μg/lane) were subjected to SDS-PAGE and transferred to PVDF membranes using the iBlot Gel Transfer system (Invitrogen). The membranes were blocked, incubated with primary antibody, washed, and incubated with the secondary HRP-labeled antibody. Bands were visualized with the ECL Prime Western blotting Detection System (GE Healthcare) and LAS-3000 (Fujifilm, Tokyo, Japan). A densitometric analysis of blotted membranes was performed using ImageJ software.

Immunoprecipitation—Immunoprecipitation of serine/threonine/tyrosine-phosphorylated proteins or lysine-acetylated proteins was carried out using the Dynabeads protein G immunoprecipitation kit (Invitrogen) according to the manufacturer's instructions. The nuclear and cytoplasmic fractions were extracted using an NE-PER nuclear and cytoplasmic extraction reagent kit (Pierce).

Detection of the Conserved Transcription Factor Binding Sites Using Multiple-genome Alignments—The Ensembl 12-way Enredo-Pecan-Ortheus (EPO) eutherian multiple alignments (12-way EPO alignments) (24, 25) were downloaded. The 12-way EPO was excised to obtain the alignment block corresponding to the human genome coordinates from 10 kb upstream of the coding sequence of *SEPP1*, including the start

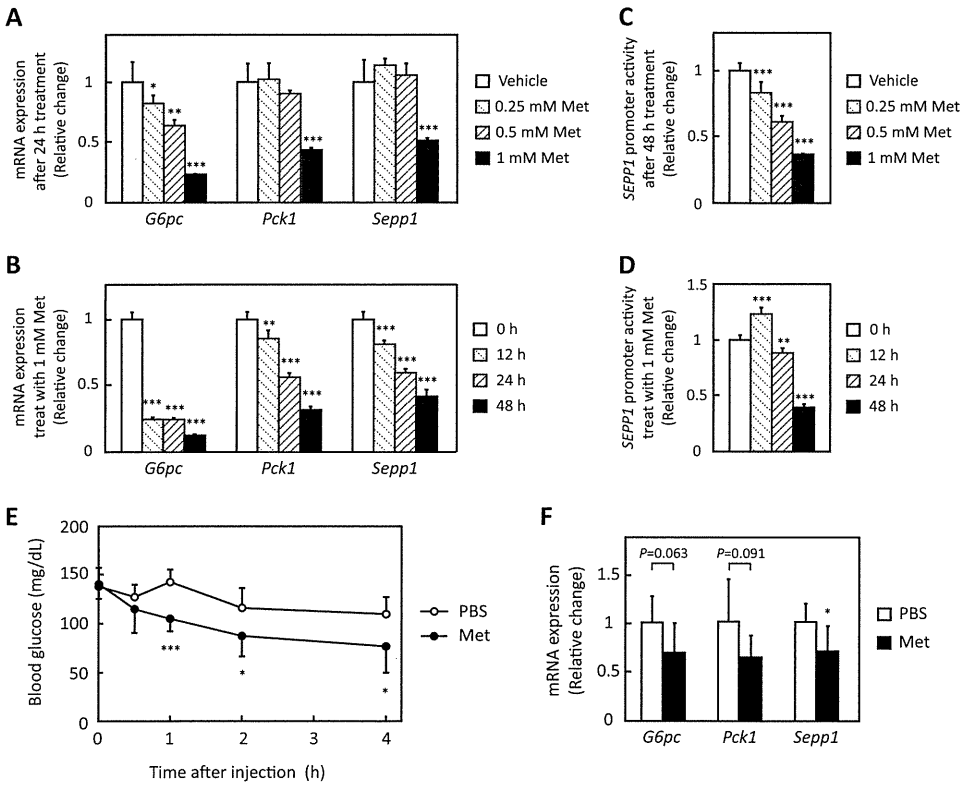

FIGURE 1. **Metformin suppressed *Sepp1* gene expression in H4IIEC3 hepatocytes and livers of C57BL/6J mice.** *A* and *B*, metformin suppressed *Sepp1* mRNA expression in a concentration- and time-dependent manner. H4IIEC3 cells were treated with the indicated concentrations of metformin for the indicated times. Expression values were normalized to *Actb* mRNA. Data represent means ± S.D. (*error bars*) ($n = 4$). *, $p < 0.05$; **, $p < 0.01$; ***, $p < 0.001$ *versus* vehicle-treated cells or 0 h. *C* and *D*, *SEPP1* promoter activity was suppressed in a concentration- and time-dependent manner. H4IIEC3 cells were co-transfected with the *SEPP1* promoter reporter vector and control reporter vector. 24 h later, the cells were treated with the indicated concentrations of metformin for the indicated times. Values were normalized to the activity of the control luciferase vector. Data represent means ± S.D. ($n = 4$). **, $p < 0.01$; ***, $p < 0.001$ *versus* vehicle-treated cells or 0 h. *E* and *F*, metformin suppressed *Sepp1* mRNA expression in livers of C57BL/6J mice. Following fasting for 4 h, 12-week-old female C57BL/6J mice were administrated 300 mg/kg metformin. 4 h after metformin administration, mice were sacrificed, and liver mRNA expression was examined. Expression values were normalized to *Actb* mRNA. Data represent means ± S.D. ($n = 7$). *, $p < 0.05$ *versus* PBS-injected mice.

codon. To predict the conserved transcription factor binding sites (TFBSs), the 10-kb upstream genome sequence for each of the 12 species was searched using the TRANSFAC (26) and the MATCH^{TM} program (27) (version 6.1) with varied thresholds. Then the predicted TFBSs were mapped on the alignments, and the conserved TFBSs for *SEPP1* were identified.

Chromatin Immunoprecipitation (ChIP) Assay—A ChIP assay was carried out using the ChIP IT Express enzymatic kit (Active Motif, Carlsbad, CA) according to the manufacturer's instructions. In brief, HepG2 cells were treated with metformin 6 h before being fixed and homogenized. Following centrifugation, the supernatant was used for chromatin samples. Chromatin samples were incubated with protein G-coated magnetic beads and ChIP grade FoxO1 or FoxO3a antibodies (Abcam, Cambridge, MA) overnight at 4 °C. Following washing and elution, a reaction solution was used as the template for PCR. PCR primers were set for amplification of the Mut-DΔ2 region of the *SEPP1* promoter, as follows: forward, 5′-GCACTTGCTACTTTCTTTTAAGTTG-3′; reverse, 5′-CACAGCAGCACACTCTGATATTTAT-3′.

Animals—12-week-old C57BL/6J female mice were obtained from CLEA Japan, Inc. (Tokyo, Japan). All animals were housed in a 12-h light/dark cycle and allowed free access to food and water. Following the fasting for 4 h, mice were administrated 300 mg/kg metformin. 4 h later, mice were anesthetized and sacrificed to allow isolation of liver tissue.

Statistical Analysis—Results are expressed as means ± S.D. Significance was tested by one-way analysis of variance with the Bonferroni method, and differences were considered statistically significant at a p value of less than 0.05.

RESULTS

Metformin Suppresses SEPP1 Expression at the Promoter Level—The effects of metformin on *Sepp1* expression in H4IIEC3 hepatocytes were examined. Metformin suppressed *Sepp1* mRNA expression in a concentration- and time-dependent manner, similarly to *G6pc* and *Pck1*, which encode representative gluconeogenic enzymes glucose-6-phosphatase and phosphoenolpyruvate carboxykinase 1, respectively (Fig. 1, *A* and *B*). These results are consistent with a previous report using rat primary hepatocytes (28). Next, the effects of metformin on *SEPP1* promoter activity were examined. The human *SEPP1* promoter region was cloned to a luciferase reporter vector as reported previously (21). The present sequence completely corresponded to the reference sequence of the National Center for Biotechnology Information, but it missed one thymidine against the sequence of the previous report (accession number Y12262) (supplemental Fig. S1). Similar to the mRNA results,

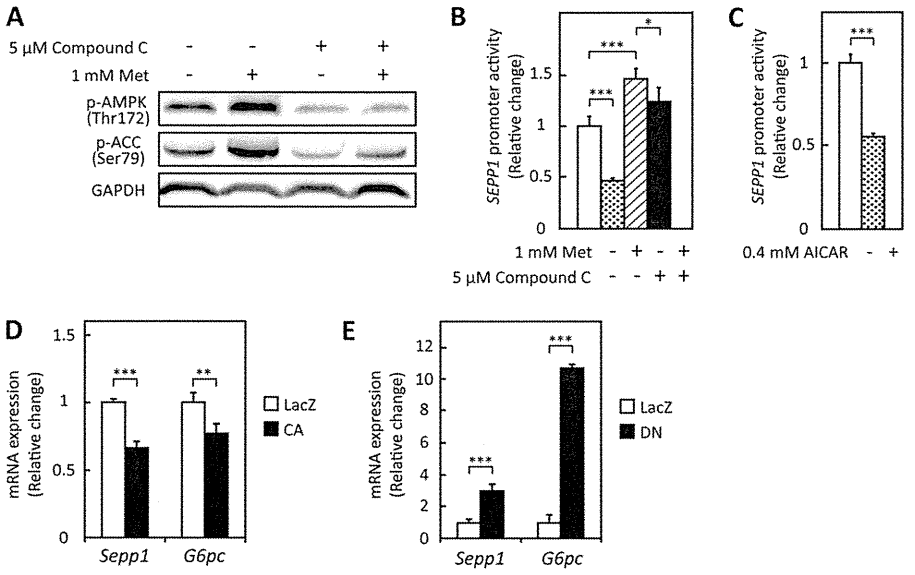

FIGURE 2. **Metformin suppressed *SEPP1* promoter activity via AMPK pathway in H4IIEC3 hepatocytes.** *A*, metformin-induced AMPK phosphorylation in the absence or presence of compound C. H4IIEC3 cells were treated with the indicated concentrations of metformin and compound C for 24 h. AMPK phosphorylation was examined by Western blotting. *B*, compound C treatment recovered metformin-induced suppression of the *SEPP1* promoter. H4IIEC3 cells were co-transfected with the *SEPP1* promoter reporter vector and control reporter vector at 24 h and then treated with the indicated concentrations of metformin and compound C for 48 h. Signals were normalized to the control reporter vector. Data represent means ± S.D. (*error bars*) ($n = 4$). ***, $p < 0.001$. *C*, AICAR suppressed *SEPP1* promoter activity. H4IIEC3 cells were co-transfected with the *SEPP1* promoter reporter vector and control reporter vector at 24 h and then treated with 0.4 mM AICAR for 24 h. Signals were normalized to the control reporter vector. Data represent means ± S.D. ($n = 4$). ***, $p < 0.001$. *D* and *E*, influence of adenoviruses carrying constitutive active (CA) or dominant negative (DN) AMPK. H4IIEC3 cells were infected with adenoviruses encoding CA-AMPK, DN-AMPK, or LacZ. Expression values were normalized to *Actb* mRNA. Data represent means ± S.D. ($n = 4$). **, $p < 0.01$; ***, $p < 0.001$.

metformin suppressed *SEPP1* promoter activity in a concentration- and time-dependent manner (Fig. 1, *C* and *D*), suggesting that it directly decreases *SEPP1* transcriptional activity in H4IIEC3 hepatocytes.

To confirm whether the present experimental condition (DMEM plus 10% FBS) supplied selenium sufficiently to synthesize selenoproteins for cultured cells, cGPx activity was measured with or without additional selenium supplement. Supplemental Fig. S2 indicates that supplementation of 100 or 1000 nM selenious acid to DMEM plus 10% FBS increased cGPx activity more than 3 times, suggesting that our experimental condition was insufficient to maximize selenoprotein synthesis. However, the current activity of cGPx in the cells cultured at DMEM plus 10% FBS (233 units/g) corresponded to the levels reported previously in the normal rat liver tissue (120–1800 units/g) (29, 30). Because these results suggest that the culture condition of DMEM plus 10% FBS was physiological, we used this condition in the following cellular experiments.

The action of metformin on *Sepp1* was also examined in mice. Following fasting for 4 h, 12-week-old female C57BL/6J mice were administrated 300 mg/kg metformin. Metformin decreased blood glucose levels by 30% (Fig. 1*E*) and tended to down-regulate gene expression for *G6pc* and *Pck1* after 4 h. Gene expression of *Sepp1* was significantly decreased by metformin (Fig. 1*F*). These results indicate that metformin suppresses gene expression for *Sepp1* in the liver of mice as well as in the cultured hepatocytes.

Metformin Suppresses SEPP1 Promoter Activity via AMPK Activation—Metformin is known to exert anti-diabetic effects by activating AMPK pathways (31). Hence, to determine whether AMPK pathways are involved in the metformin-induced suppression of *SEPP1* promoter activity, cells were treated with compound C, a representative AMPK inhibitor. Findings confirmed that the metformin-induced phosphorylation of AMPK and acetyl-CoA carboxylase was cancelled by the co-administration of compound C in H4IIEC3 hepatocytes (Fig. 2*A*). Co-administration of compound C partly rescued the cells from the inhibitory effects of metformin on the *SEPP1* promoter (Fig. 2*B*) and increased *SEPP1* promoter activity in the absence of metformin (Fig. 2*B*). In contrast, treatment with AICAR, a known activator of AMPK, decreased *SEPP1* promoter activity similarly to metformin (Fig. 2*C*). To determine whether AMPK pathways were involved in *SEPP1* promoter activity, H4IIEC3 hepatocytes were infected with an adenovirus encoding CA- or DN-AMPK. Transfection with CA-AMPK suppressed *Sepp1* and *G6pc* mRNA expression (Fig. 2*D*), whereas transfection with DN-AMPK enhanced *Sepp1* and *G6pc* mRNA expression (Fig. 2*E*). These results suggest that metformin decreases *SEPP1* promoter activity, at least partly, by activating AMPK.

Metformin-response Element in the SEPP1 Promoter Includes the FoxO Binding Site—To determine the nature of the metformin-response element in the *SEPP1* promoter region, several deletion mutants of the *SEPP1* promoter were constructed (Fig. 3*A*). Promoter activity of Mut-A to Mut-D, but not Mut-E, was suppressed by metformin treatment (Fig. 3*A*), indicating that the metformin-response element of the *SEPP1* promoter exists in Mut-D. Additional deletion mutants of Mut-D were constructed and named Mut-DΔ1 to DΔ3. Mut-DΔ1 and -DΔ2, but not Mut-DΔ3, were suppressed by metformin (Fig. 3*B*), indicating that the metformin-response element in the *SEPP1* promoter is localized in the Mut-DΔ2 sequence. Using computational analysis to identify conserved TFBSs among the species (see "Experimental Procedures"), several putative TFBSs were identified in the Mut-DΔ2 sequence (supplemental Fig. S3).

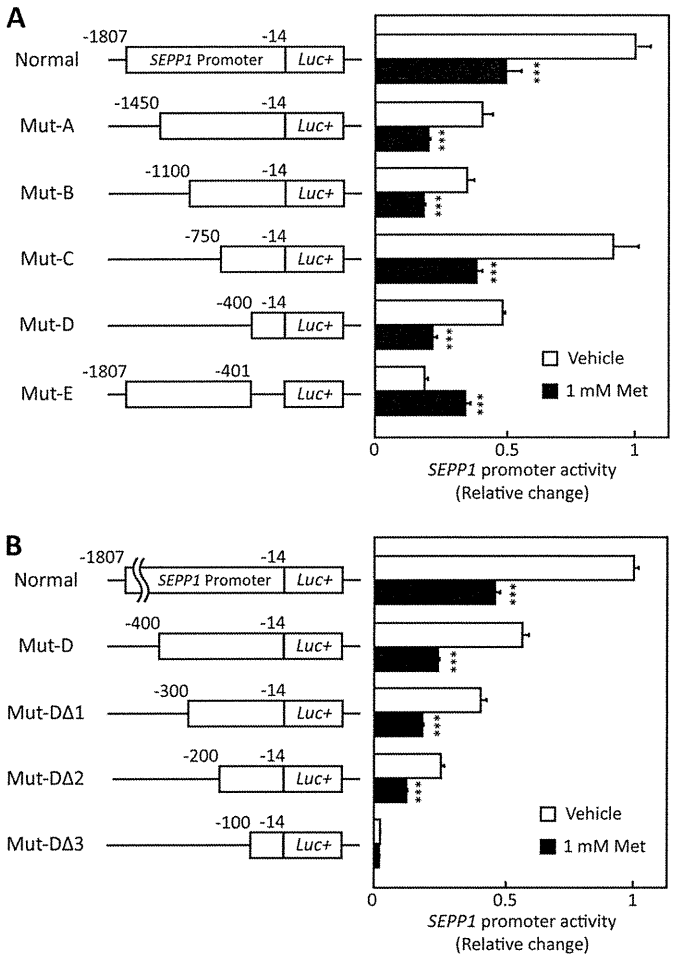

FIGURE 3. **SEPP1 promoter activity of deletion mutants.** *A* and *B*, structure and luciferase activity of promoter-deletion mutants. The sequences deleted within the constructs are shown as *thin lines*. The remaining parts of the *SEPP1* promoter were fused to a luciferase reporter gene. H4IIEC3 cells were co-transfected with each reporter vector and control reporter vector at 24 h and then treated with the indicated concentrations of metformin for 48 h. Signals were normalized to the control reporter vector. Data represent means ± S.D. (*error bars*) ($n = 4$). ***, $p < 0.001$ *versus* vehicle-treated cells.

Because early reports indicate that AMPK directly phosphorylates FoxO3a and regulates its transcriptional activity (16), this investigation focused on the two putative FoxO binding sites (Fig. 4*A*).

Metformin Suppresses FoxO Activity via AMPK Activation—To determine whether metformin treatment influences FoxO activity, a forkhead-response element (FHRE)-Luc vector that includes three tandems of FHREs ligated with a luciferase gene was utilized (32). This vector was used as a reporter of FoxO-responsive promoter activity (33). Metformin treatment suppressed FHRE activity, and concurrent treatment with compound C completely cancelled this suppression (Fig. 4*B*). In addition, treatment with compound C stimulated FHRE activity in the absence of metformin (Fig. 4*B*), whereas AICAR treatment suppressed FHRE activity (Fig. 4*C*). These results suggest that metformin suppresses FHRE activity via AMPK activation. To determine the critical FoxO binding site for metformin-induced *SEPP1* suppression, we constructed luciferase vectors that deleted either of two putative FoxO binding sites and were named Mut-DΔ2-ΔFoxo A or B, respectively (supplemental Fig. S4). Luciferase assay using these vectors revealed that putative FoxO binding site B was essential for metformin-induced *SEPP1* suppression (Fig. 4*D*). Because the assays using these vectors are not specific to FoxO3a activity, the interaction of FoxO proteins with DNA sequences in the *SEPP1* promoter was examined using a ChIP assay. For the ChIP assay, HepG2 cells were utilized to evaluate the human *SEPP1* promoter. Metformin suppressed *SEPP1* expression in HepG2 cells as well as H4IIEC3 cells (data not shown). The ChIP assay indicates that treatment with metformin decreased the binding of FoxO3a to *SEPP1* promoter, whereas it increased the binding of FoxO1 (Fig. 4*E*). These results suggest that FoxO3a, but not FoxO1, is associated with the metformin-induced suppression of *SEPP1* expression.

Metformin Suppresses SEPP1 Expression via FoxO3a Inactivation—Next, we examined whether the specific knockdown of endogenous *Foxo3a* or *Foxo1* affects *Sepp1* expression in H4IIEC3 hepatocytes. Transfection with *Foxo3a*- or *Foxo1*-specific siRNA resulted in a ~50% reduction in mRNA levels of *Foxo3a* or *Foxo1* (Fig. 5*A*). Knockdown of both *Foxo1* and *Foxo3a* resulted in a significant down-regulation of *Sepp1* expression (Fig. 5*A*). Interestingly, mRNA levels of *G6pc* were decreased by *Foxo3a* knockdown (Fig. 5*A*), suggesting that not only FoxO1 but also FoxO3a positively regulates the expression of the gluconeogenesis-related genes in H4IIEC3 hepatocytes. Next, we assessed whether knockdown of *Foxo3a* selectively affects the inhibitory action of metformin on the *SEPP1* promoter. Transfection with siRNAs for *Foxo3a*, but not for *Foxo1*, cancelled metformin-induced suppression of Mut-DΔ2 luciferase activity (Fig. 5*B*). These results suggest that the metformin-induced suppression of *Sepp1* is dependent on FoxO3a but not on FoxO1.

Whether FoxO3a overexpression influences the action of metformin on *SEPP1* promoter activity was also investigated. The FoxO3a protein was overexpressed in a concentration-dependent manner in cells transfected with the pCMV6-FoxO3a expression vector (Fig. 5*C*). Overexpression of FoxO3a significantly enhanced *SEPP1* promoter activity (Fig. 5*D*), and transfection with pCMV6-FoxO3a rescued the cells from the suppressive effect of metformin on *SEPP1* promoter activity in a concentration-dependent manner (Fig. 5, *D* and *E*). These results indicate that metformin decreases *SEPP1* promoter activity and gene expression via FoxO3a inactivation in H4IIEC3 hepatocytes.

Metformin Decreases FoxO3a Protein in the Nuclear Components—To elucidate the mechanism by which metformin inactivates FoxO3a, phosphorylation and acetylation of FoxO3a were examined in hepatocytes treated with metformin. Metformin treatment altered neither mRNA levels of *Foxo3a* (Fig. 6*A*) nor protein levels of FoxO3a (Fig. 6*B*). However, immunoprecipitation experiments revealed that treatment with metformin phosphorylated FoxO3a but not FoxO1 in H4IIEC hepatocytes (Fig. 6, *B* and *C*, and supplemental Fig. S5). Because a previous report indicated that FoxO3a, as well as FoxO1, is deacetylated by sirtuin family proteins downstream of AMPK (34), we examined the deacetylation of FoxO3a and FoxO1. Acetylation of both FoxO1 and FoxO3a was unaffected by metformin administration (Fig. 6, *B* and *C*, and supplemental Fig. S5). To determine the intracellular localization of FoxO3a, the cytosolic and

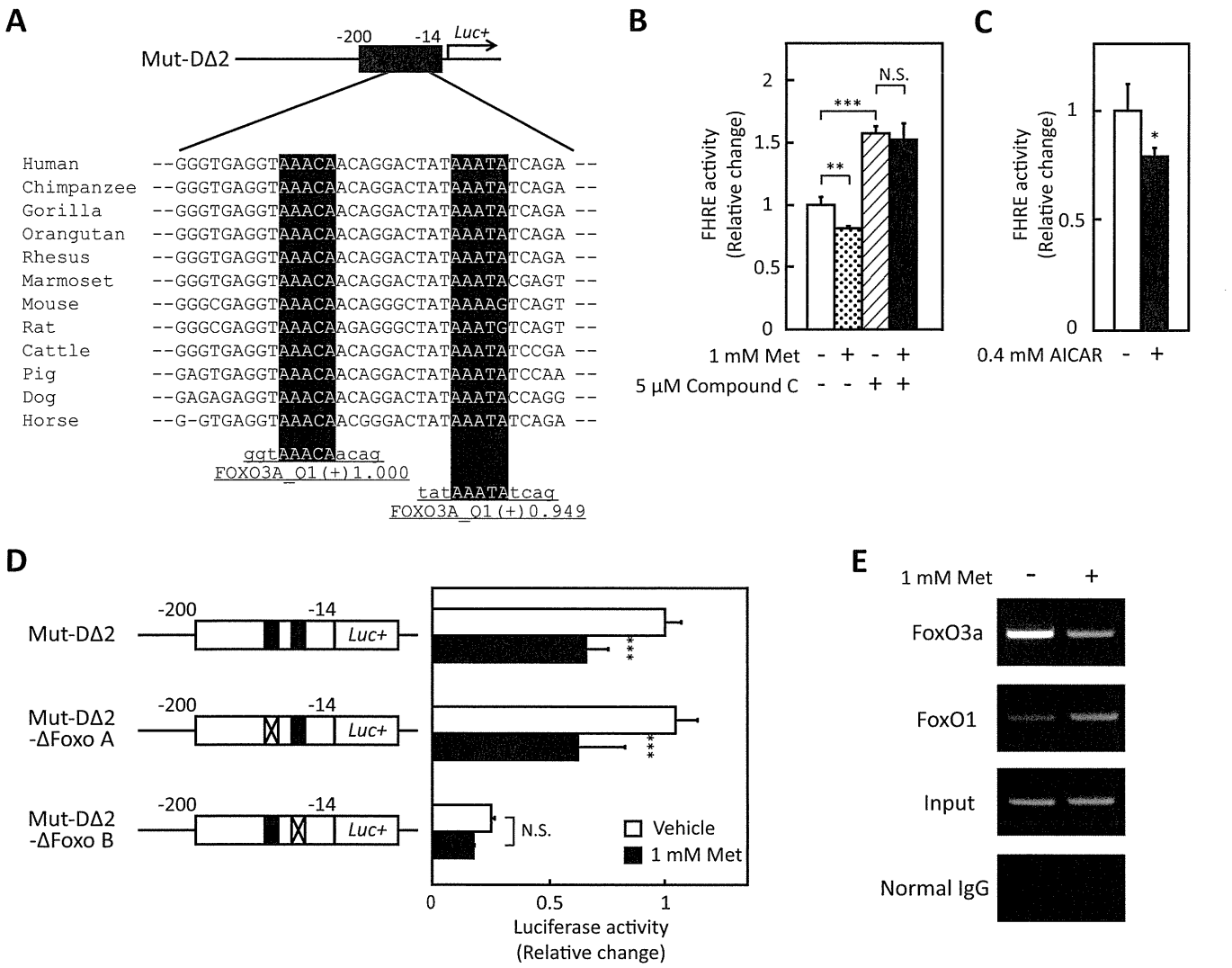

FIGURE 4. **Activation of the AMPK suppressed FoxO activity.** *A*, putative FoxO3a binding sites of Mut-DΔ2 sequence. Detection of the conserved TFBSs was performed using multiple-genome alignments and the *highlighted* putative transcriptional factor binding sites. *B*, FoxO activity in the absence or presence of metformin and compound C. H4IIEC3 cells were co-transfected with the FHRE-Luc vector and control reporter vector at 24 h and then treated with the indicated concentrations of metformin and compound C for 48 h. Signals were normalized to the control reporter vector. Data represent means ± S.D. (*error bars*) ($n = 4$). **, $p < 0.01$; ***, $p < 0.001$. *N.S.*, not significant. *C*, FoxO activity in the absence or presence of AICAR. H4IIEC3 cells were co-transfected with the FHRE-Luc vector and control reporter vector at 24 h and then treated with the indicated concentrations of AICAR for 24 h. Signals were normalized to the control reporter vector. Data represent means ± S.D. ($n = 4$). *, $p < 0.05$ *versus* vehicle-treated cells. *D*, deficiency of putative FoxO binding site cancelled metformin-induced suppression of *SEPP1* promoter activity. H4IIEC3 cells were co-transfected with each reporter vector and control reporter vector at 24 h and then treated with the indicated concentrations of metformin for 24 h. Signals were normalized to the control reporter vector. Data represent means ± S.D. ($n = 4$). ***, $p < 0.001$ *versus* vehicle-treated cells. *E*, chromatin immunoprecipitation assay of HepG2 cells treated with metformin. HepG2 cells were treated with metformin for 6 h. Chromatin samples precipitated with anti-FoxO3a, anti-FoxO1, or normal IgG were amplified using primers for the Mut-DΔ2 region of the human *SEPP1* promoter.

nuclear components of the FoxO3a protein were fractionated. FoxO3a and FoxO1 protein levels were decreased by metformin treatment in the nuclear fraction (Fig. 6*D*). These results suggest that metformin inactivates FoxO3a by decreasing FoxO3a protein levels in the nucleus and subsequently inhibiting the binding of FoxO3a to the *SEPP1* promoter.

DISCUSSION

Our data demonstrate that metformin suppresses production of the insulin resistance-inducing hepatokine SeP by activating AMPK and subsequently inactivating FoxO3a in H4IIEC3 hepatocytes. During the course of this study, it was reported that metformin decreases mRNA levels of *Sepp1* in rat primary hepatocytes (28); however, the molecular mechanisms by which metformin reduces the expression of *Sepp1* were not fully understood. Our data demonstrate that the AMPK/FoxO3a pathway downstream of metformin action plays a major role in the regulation of *SEPP1* expression in cultured hepatocytes. Our data suggest a previously unrecognized mechanism of action of metformin in combating the systemic insulin resistance in type 2 diabetes.

The finding that FoxO3a positively regulates *Sepp1* and *G6pc* expression in H4IIEC3 hepatocytes supports the suggestion that FoxO3a plays an important role in glucose homeostasis. The ability of FoxO1 to increase the expression of gluconeogenic genes has been confirmed (35). To date, however, little

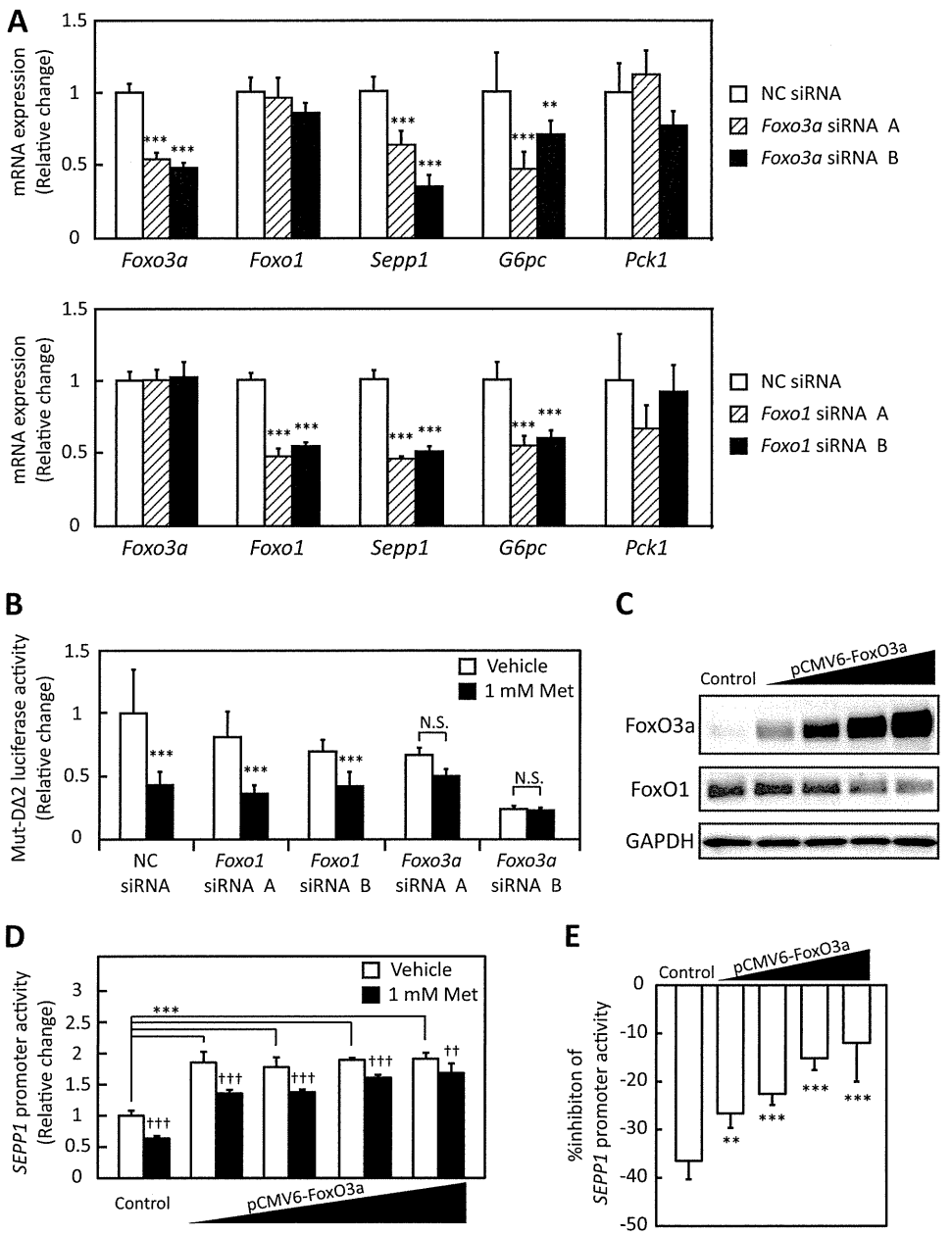

FIGURE 5. **Metformin suppressed SeP expression via FoxO3a.** *A*, efficiency of *Foxo3a* siRNA and *Foxo1* siRNA. H4IIEC3 cells were transfected with *Foxo3a* siRNAs or *Foxo1* siRNAs or a negative control (*NC*) siRNA at 48 h. Knockdown efficiency was assessed by real-time PCR. Expression values were normalized to *Actb* mRNA. Data represent means ± S.D. (*error bars*) ($n = 4$). **, $p < 0.01$; ***, $p < 0.001$ *versus* negative control siRNA-treated cells. *B*, luciferase activity of Mut-DΔ2 treated with *Foxo3a* or *Foxo1* siRNA and metformin. H4IIEC3 cells were transfected with *Foxo3a* siRNAs or *Foxo1* siRNAs or negative control siRNA at 24 h and then co-transfected with Mut-DΔ2 vector and control reporter vector. 24 h after transfection, cells were treated with the indicated concentrations of metformin for 24 h. Signals were normalized to the control reporter vector. Data represent means ± S.D. ($n = 4$). ***, $p < 0.001$ *versus* vehicle-treated cells. *N.S.*, not significant. *C*, protein levels in the presence of the FoxO3a overexpression vector. H4IIEC3 cells were transfected with the pCMV-FoxO3a vector or pCMV empty vector at 24 h. FoxO3a protein levels were then assessed by Western blotting. *D*, *SEPP1* promoter activity transfected with the FoxO3a overexpression vector. H4IIEC3 cells were co-transfected with the expression vectors for FoxO3a, *SEPP1* promoter reporter and control reporter at 24 h and then treated with the indicated concentrations of metformin for 48 h. Data represent means ± S.D. ($n = 3$–4). ***, $p < 0.001$ *versus* control; ††, $p < 0.01$; †††, $p < 0.001$ *versus* vehicle-treated cells. *E*, percentage inhibition of *SEPP1* promoter activity by metformin. Suppression ratios of *SEPP1* promoter activity were calculated based on the data in *E*. Data represent means ± S.D. ($n = 3$–4). **, $p < 0.01$; ***, $p < 0.001$ *versus* control.

information concerning the involvement of FoxO3a in glucose metabolism is available. Certainly, no defects in glucose metabolism have been described in FoxO3a-deficient mice (36), suggesting that the function of FoxO3a in glucose metabolism is compensated for by FoxO1. Indeed, Haeusler *et al.* (37) reported that triple liver-specific ablation of FoxO1, FoxO3a, and FoxO4 causes a more pronounced hypoglycemia and increased insulin sensitivity in mice compared with a single knockout of FoxO1. The present findings indicate that FoxO proteins, including FoxO3a, regulate hepatic glucose metabolism in a coordinated manner. These data reveal that FoxO3a, the downstream target of metformin/AMPK, positively regulates *SEPP1* transcriptional activity in cultured hepatocytes independently of FoxO1 and suggest that